

การกักเก็บน้ำมันกานพลูที่กระจายตัวในน้ำในบีดแอลจินตและในฟิล์มเซลลูโลส



นางสาวปิยวรา ตั้งอิธิบาท

จุฬาลงกรณ์มหาวิทยาลัย

CHULALONGKORN UNIVERSITY

บทคัดย่อและแฟ้มข้อมูลฉบับเต็มของวิทยานิพนธ์ตั้งแต่ปีการศึกษา 2554 ที่ให้บริการในคลังปัญญาจุฬาฯ (CUIR)

เป็นแฟ้มข้อมูลของนิสิตเจ้าของวิทยานิพนธ์ ที่ส่งผ่านทางบัณฑิตวิทยาลัย

The abstract and full text of theses from the academic year 2011 in Chulalongkorn University Intellectual Repository (CUIR) are the thesis authors' files submitted through the University Graduate School.

วิทยานิพนธ์นี้เป็นส่วนหนึ่งของการศึกษาตามหลักสูตรปริญญาวิทยาศาสตรมหาบัณฑิต

สาขาวิชาเคมี ภาควิชาเคมี

คณะวิทยาศาสตร์ จุฬาลงกรณ์มหาวิทยาลัย

ปีการศึกษา 2559

ลิขสิทธิ์ของจุฬาลงกรณ์มหาวิทยาลัย

ENCAPSULATION OF WATER-DISPERSED CLOVE OIL IN ALGINATE BEADS AND
CELLULOSE FILMS

Miss Peewara Tungittibath



A Thesis Submitted in Partial Fulfillment of the Requirements
for the Degree of Master of Science Program in Chemistry

Department of Chemistry

Faculty of Science

Chulalongkorn University

Academic Year 2016

Copyright of Chulalongkorn University

ปียวรา ตั้งอธิบาท : การกักเก็บน้ำมันกานพลูที่กระจายตัวในน้ำในบีดแอลจิเนตและในฟิล์มเซลลูโลส (ENCAPSULATION OF WATER-DISPERSED CLOVE OIL IN ALGinate BEADS AND CELLULOSE FILMS) อ.ที่ปรึกษาวิทยานิพนธ์หลัก: ผศ. ดร.พัฒนรา ธีรพิบูลย์เดช, 53 หน้า.

งานวิจัยนี้มีวัตถุประสงค์เพื่อเตรียมฟิล์มน้ำมันกานพลูและเม็ดบีดน้ำมันกานพลูเพื่อใช้เป็นยาสลบปลา ทั้งสองรูปแบบอยู่บนพื้นฐานของการรวมตัวกันของน้ำมันกานพลูในเมทริกซ์ของคาร์บอกซีเมทิลเซลลูโลสและแซนแทนกัม เพื่อเพิ่มความสามารถในการละลายน้ำของน้ำมันกานพลูในน้ำและน้ำทะเล ค่าเปอร์เซ็นต์ประสิทธิภาพของการกักเก็บน้ำมันกานพลูของแผ่นฟิล์มและเม็ดบีดอยู่ที่ 32.7 และ 8.0 ตามลำดับ แผ่นฟิล์มน้ำมันกานพลูละลายในน้ำได้ดีกว่าในน้ำทะเล ในขณะที่เม็ดบีดน้ำมันกานพลูมีการบวมตัวได้เร็วกว่าเมื่ออยู่ในน้ำทะเลแต่มีการปลดปล่อยเร็วกว่าเมื่ออยู่ในน้ำ ภาพถ่ายจากกล้องจุลทรรศน์อิเล็กตรอนไมโครสโคปแบบส่องกราด อินฟราเรดสเปกตรัม และ TGA เทอร์โมแกรมยืนยันได้อย่างชัดเจนว่ามีน้ำมันกานพลูอยู่ในเครือข่ายของพอลิเมอร์เมทริกซ์ แผ่นฟิล์มและเม็ดบีดน้ำมันกานพลูถูกเก็บรักษาในการซีลแบบสุญญากาศและไม่มีสุญญากาศที่อุณหภูมิ 40 องศาเซลเซียสเป็นเวลา 120 วันและตรวจสอบคุณสมบัติทางเคมีและทางกายภาพ ลักษณะสีของทั้งสองรูปแบบจะค่อยๆเหลืองขึ้น ค่าเปอร์เซ็นต์ประสิทธิภาพของการกักเก็บน้ำมันกานพลูของแผ่นฟิล์มลดลงแต่เม็ดบีดน้ำมันกานพลูไม่มีการเปลี่ยนแปลงในทั้งสองสภาวะ คุณสมบัติส่วนใหญ่ของทั้งสองรูปแบบไม่แตกต่างกันอย่างมีนัยสำคัญระหว่างสภาวะสุญญากาศและสภาวะที่ไม่สุญญากาศ

จุฬาลงกรณ์มหาวิทยาลัย
CHULALONGKORN UNIVERSITY

ภาควิชา เคมี

ลายมือชื่อนิสิต

สาขาวิชา เคมี

ลายมือชื่อ อ.ที่ปรึกษาหลัก

ปีการศึกษา 2559

5772062823 : MAJOR CHEMISTRY

KEYWORDS: CLOVE OIL / CELLULOSE FILM / ALGINATE BEAD / SOLUBILITY

PEEWARA TUNGITTIBATH: ENCAPSULATION OF WATER-DISPERSED CLOVE OIL IN ALGINATE BEADS AND CELLULOSE FILMS. ADVISOR: ASST. PROF. PATTARA THIRAPHIBUNDET, Ph.D., 53 pp.

The aim of this research was to prepare of clove oil (CO) film and clove oil-loaded alginate bead to use as fish anesthetic. Both forms were based on the incorporation of clove oil in the matrix of carboxymethylcellulose (CMC) and xanthan gum (XG) to enhance the water solubility of CO in the water and seawater. The loading efficiencies of CO film and bead were 32.7% and 8.0%, respectively. The CO films dissolve in water better than that in the seawater, whereas CO-loaded alginate bead swelled faster in the seawater but released faster in the water. The SEM images, IR spectrum and TGA thermograms clearly confirmed the presence of clove oil in the network of polymer matrix. The CO film and bead were kept in vacuum and non-vacuum foil sealed bag at 40°C for 120 days. Their chemical and physical properties were investigated. The color of both forms was gradually yellow. The LC percentage of CO film was reduced but that of CO bead unchanged in both conditions. Most properties of both forms were not significantly different between storage in vacuum and non-vacuum.

Department: Chemistry

Student's Signature

Field of Study: Chemistry

Advisor's Signature

Academic Year: 2016

ACKNOWLEDGEMENTS

Firstly, I would like to express my sincere gratitude to my advisor Assistant Professor Pattara Thiraphibundet, Ph.D., for her valuable advice, supervision and assistance throughout the course of this research. I am also grateful thank to the member of thesis committee consist of Associate Professor Vudhichai Parasuk, Ph.D., Assistant Professor Varawut Tangpasuthadol, Ph.D. and Assistant Professor Nalena Praphairaksit, D.V.M., Ph.D. the external examiner from Faculty of Science, Srinakharinwirot University, for their valuable comments and suggestions.

I am forever thankful to PAT group, Department of Chemistry, Faculty of Science, Chulalongkorn University for their friendship and support, and for creating a cordial working environment. and I have many, many people to thank for listening to and, at times, having to tolerate me over the past three years.

Finally, my deep and sincere gratitude to my family for their continuous and unparalleled love, help and support. They selflessly encouraged me to explore new directions in life and seek my own destiny. This journey would not have been possible if not for them.

CONTENTS

	Page
THAI ABSTRACT	iv
ENGLISH ABSTRACT	v
ACKNOWLEDGEMENTS	vi
CONTENTS	vii
LIST OF TABLES	xi
LIST OF FIGURES	xii
LIST OF ABBREVIATION.....	xiv
CHAPTER I.....	1
Introduction	1
1.1 Motivation of research	1
CHAPTER II.....	3
THEORY AND LITERATURE REVIEWS	3
2.1 Clove oil.....	3
2.2 Fish anesthetic.....	4
2.3 Improvement solubility of clove oil.....	6
2.4 Edible film.....	6
2.5 Alginate bead	11
CHAPTER III.....	13
EXPERIMENTAL	13
3.1 Chemicals and materials	13
3.2 Chemical stability of clove oil.....	13
3.3 Preparation of film	13

	Page
3.4 Physical properties of films	14
3.4.1 Thickness	14
3.4.2 Water solubility	15
3.4.3 Color	15
3.4.4 Moisture content	16
3.4.5 Scanning electron microscopy (SEM)	16
3.4.6 Thermal gravimetric analysis (TGA)	16
3.4.7 Fourier transformed infrared (FTIR) spectroscopy	16
3.5 Solubility of clove oil	16
3.6 Preparation of beads	17
3.7 Swelling study	18
3.8 Release study	19
3.9 Physical properties of beads	19
3.9.1 Size	19
3.9.2 Moisture content	19
3.9.3 Scanning electron microscopy (SEM)	20
3.9.4 Fourier transformed infrared (FTIR) spectroscopy	20
3.10 Stability study	20
CHAPTER IV	21
RESULT AND DISCUSSION	21
4.1. Chemical stability of clove oil	21
4.2 Entrapment efficiency (EE) and loading capacity (LC) of clove oil films	21
4.3 Characterization of CO film	23

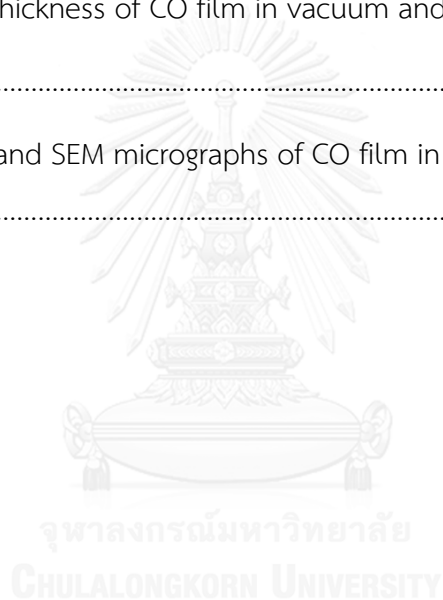
	Page
4.3.1 Appearance, color and thickness	23
4.3.2 Water solubility and moisture content	23
4.3.3 Microstructure of films.....	24
4.3.4 Fourier-transform infrared (FTIR) spectroscopy	25
4.3.5 Thermal stability	26
4.4 Water solubility of clove oil and clove oil in film.....	27
4.5 Preparation of beads	28
4.5.1 Swelling and releasing study	28
4.5.2 Morphology of the beads	30
4.5.3 Fourier-transform infrared (FTIR) spectroscopy	30
4.6 Shelf-life stability of CO film.....	31
4.6.1 Appearance, color and thickness	31
4.6.2 LC percentage and SEM analysis CO film in vacuum and non-vacuum conditions.....	33
4.6.3 Solubility and moisture content.....	33
4.6.4 Thermal stability	35
4.6.5 Fourier-transform infrared (FTIR) spectroscopy	36
4.7 Stability of CO beads.....	37
4.7.1 Appearance and size	37
4.7.2 Loading capacity percentage, SEM analysis and moisture content	39
4.7.3 Fourier-transform infrared (FTIR) spectroscopy	40
CHAPTER V	41
CONCLUSION	41

	Page
REFERENCES	43
APPENDIX.....	49
Appendix A.....	50
Appendix B.....	51
Appendix C.....	52
VITA.....	53



LIST OF TABLES

Table	Page
3.1 Compositions of film-forming polymers used for preparing clove oil film	14
3.2 Compositions of mixture for preparing clove oil beads	18
4.1 The LC and EE percentages of the CO films by varying the XG concentrations....	22
4.2 The LC and EE percentages of the $C^2X^{0.8}$ film by varying the CO concentration ..	22
4.3 Appearance and thickness of CO film in vacuum and non-vacuum conditions	32
4.4 Appearance, size and SEM micrographs of CO film in vacuum and non-vacuum conditions.....	38



LIST OF FIGURES

Figure	Page
2.1 Chemical structures of a) eugenol, b) eugenyl acetate and c) β -caryophyllene.....	4
2.2 Plasma cortisol concentrations of channel catfish during 30-minute anesthetization with 100 ppm TMS, 30 ppm quinaldine, 100 ppm clove oil and 6 ppm metomidate	5
2.3 Mechanisms of anaesthesia.....	6
2.4 Dip coating process	8
2.5 Spray coating	8
2.6 Spin coating process	9
2.7 Solvent casting process	9
2.8 Chemical structures of a) carboxymethyl cellulose and b) xanthan gum	11
2.9 Chemical structures of G blocks, M blocks and MG blocks in alginate.....	11
2.10 Binding to calcium ions by G-block in alginate and Egg-box model structure of an alginate gel formation.....	12
4.1 The NMR spectrum of a) clove oil and b) 1-year clove oil	21
4.2 a) control film and b) CO film.....	23
4.3 The solubility of control and CO film at a) 20 ppm and b) 50 ppm of CO in film	24
4.4 SEM micrographs of the surfaces (left column, A) and cross-sections (right column, B) of the a) control film and b) CO film	25
4.5 FTIR spectra of a) CO b) control film and c) CO film.....	26
4.6 TGA curves and DTG thermograms of a) CMC, b) XG, c) control film and d) CO film.....	27

4.7	The solubility of CO and CO film in water and seawater	27
4.8	Swelling profiles of the six types of alginate beads in water at the interval times	28
4.9	Swelling profiles of the CO beads in water and seawater for 180 minutes.....	29
4.10	Cumulative release of CO in water and seawater for 180 minutes.....	29
4.11	Photos of a. control beads and b. CO beads by a digital camera.....	30
4.12	SEM micrographs of the surfaces (left, A) and cross-sections (right, B) of the a) control bead and b) CO bead.....	30
4.13	FTIR spectrum of a) CO, b) control bead and c) CO bead.	31
4.14	Color of CO film in vacuum and non-vacuum conditions.....	33
4.15	The %LC of CO film in vacuum and non-vacuum conditions.....	33
4.16	The water and seawater solubility of CO film at a) 20 and b) 50 ppm of CO within film in vacuum and non-vacuum condition	34
4.17	The moisture content of CO film in vacuum and non-vacuum condition	35
4.18	a) TGA and b) DTG thermograms of CO film after 0 day, 60 days in vacuum, 60 days in non-vacuum, 120 days in vacuum and 120 days in non-vacuum conditions.....	36
4.19	FTIR spectra of CO film at a) 0 day, b) 60 day in vacuum, c) 60 day in non- vacuum, d) 120 day in vacuum and e) 120 day in non-vacuum conditions	36
4.20	The %loading capacity of CO beads in vacuum and non-vacuum conditions....	39
4.21	The moisture content of CO beads in vacuum and non-vacuum conditions.....	39
4.22	FTIR spectra of CO beads at a) 0 day, b) 60 day in vacuum, c) 60 day in non- vacuum, d) 120 day in vacuum and e) 120 day in non-vacuum conditions	40

LIST OF ABBREVIATION

%	percentage
°C	degree celsius
β	beta position
cm^{-1}	unit of wavenumber (IR)
CMC	carboxymethyl cellulose
CO	clove oil
XG	xanthan gum
EE	entrapment efficiency
FTIR	fourier transform infrared
g	gram
mg	milligram
kg	kilogram
mmole	millimole
mL	milliliter
mm	millimeter
nm	nanometer
ppm	parts per million
cm	centimeter
wt	weight
min	minute
LC	loading capacity
μL	microliter
<i>et al.</i>	et alli, and other
SEM	scanning electron microscope
w/v	weight by volume
v/v	volume by volume
rpm	revolutions per minute
MS-222	tricaine methanesulfonate

BC	before Christ
U.S. FDA	United States food and drug administration
TGA	thermal gravimetric analysis



CHAPTER I

Introduction

1.1 Motivation of research

Clove oil is commonly obtained from the stems, leaves and flowers of *Eugenia aromatica* and *Eugenia caryophyllata* by steam distillation [1]. The main components in clove oil are eugenol, eugenyl acetate and β -caryophyllene. Clove oil possess a variety of bioactivities such as anti-cariogenic [2], anti-oxidation [3], anti-tyrosinase [3], anti-microbial [4], anti-inflammatory [5], anti-fungal [6] and anti-bacterial [7] and fish anesthesia [8] activities.

Fish anesthesia greatly facilitates surgery, transportation, examination and diagnostic sampling because anesthesia reduces stress and protects fish injury. Appropriate fish anesthetic should have short induction and recovery time, safe for human and aquatic animals, environmentally friendly and no residue in fish and consumer [9]. Nowadays, economical fish anesthetics are synthetic chemicals which are tricaine methanesulfonate (MS-222), 2-phenoxyethanol and quinaldine. However, these anesthetics are relatively expensive and regarded as carcinogenic. The withdrawal period requires up to 21 days before consumption or liberation into the nature [10]. Clove oil is the natural chemical which has been studied to use as an alternative fish anesthetic. Its advantages over commercial anesthetics are low price, less environmental impact, and safety for human. However, clove oil must be dissolved in ethanol with the ratio of 1:9 before adding in the fish tank [11]. Ethanol is

found to affect the the fish anxiety and irritation. Therefore, this research aims to increase the water dispersion of clove oil by incorporating clove oil into 2 platforms; blend film and alginate bead. The advantages of both forms are no usage of organic solvents, light weight, easy storage and easy use. Clove oil film is able to dissolve in the water and the clove oil in the matrix of film-forming polymers can disperse in the water. For the clove oil-loaded alginate bead, clove oil is incorporated in the matrix of some polymers and sodium alginate. The beads are slowly swell and release clove oil into the water.

Thus, the objective of this research is to fabricate the clove oil film and bead to use as the fish anesthetic. The clove oil is entrapped in the matrix of carboxymethyl cellulose and xanthan gum in order to increase the water dispersion. Moreover, we also study the shelf-life stability of clove oil film and bead for 120 days.

CHAPTER II

THEORY AND LITERATURE REVIEWS

2.1 Clove oil

Clove oil is an essential oil extracted from *Eugenia aromatica* and *Eugenia caryophyllata* by steam distillation. The scientific classification of clove is [1]:

Botanical Name: *Syzygium aromaticum* (L.) Merr. and L. M. Perry.

Synonyms: *Caryophyllus aromaticus* L.; *Eugenia aromatica* (L.) Baill.;
Eugenia caryophyllata Thunb.

Family: Myrtaceae.

Common Name: Clove

Clove is one of the indigenous spices in Asian countries. Clove just like many other spices originating in Asia that it has a great history behind it. The usage history of clove bud was found in China since 207 BC. Chinese emperors in the Han Dynasty used cloves to treat mouth odor. Moreover, cloves have been used to prepare many traditional Chinese medicines for treatment multiple disciplines. In Thailand, clove powders and clove oils have been used for treatment of asthma, beriberi, scurvy, flatulence, indigestion, nauseous, diarrhea, phlegm and hiccup. Clove oil obtained by the steam distillation of clove buds consists primarily of three compounds: eugenol (up to 85-95%), eugenyl acetate (up to 15%) and β -caryophyllene (up to 8%) (Fig. 2.1). Clove oil has been known for its benefits to oral health. It can be used as a dental anesthetic and as a mouthwash to help fighting mouth and throat infections [2]. Therefore, it is added to many pharmaceutical and dental products. Moreover, clove oil exhibits many bioactivities; anti-oxidation [3], anti-tyrosinase [3], anti-microbial [4], anti-inflammatory [5], anti-fungal [6] and anti-bacterial [7] and fish anesthesia [8] activities.

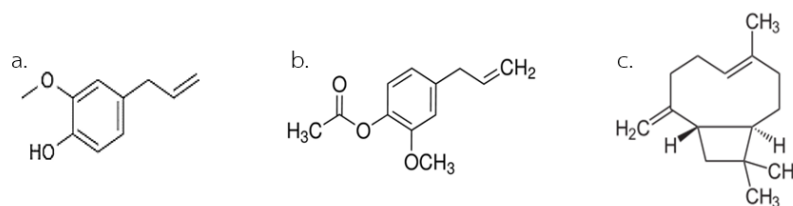


Figure 2.1 Chemical structures of a) eugenol, b) eugenyl acetate and c.) β-caryophyllene [1]

2.2 Fish anesthetic

Fish anesthetic is used for reducing trauma during surgery, handling and transportation. The important considerations of good anesthetic are efficacy, cost, availability and ease of use, as well as toxicity to fish, humans and the environment [9]. The commercial fish anesthetics are 2-phenoxyethanol, tricaine methanesulfonate (MS-222) and quinaldine. However, these anesthetics are relatively expensive and regarded as carcinogenic. Moreover, the withdrawal period is required up to 21 days before human consumption [10]. Clove oil had been studied to use as an alternative fish anesthetic since 1995 and found that clove oil is an effective anesthetic for the sedation on aquatic animals (both fresh water and sea water animals). Its advantages include little environmental impact, low price, relatively few adverse reactions, safety for staff and no accumulation in fish tissues after use for 48 hours [12]. In addition, clove oil is certified by U.S. Food and Drug Administration (U.S.FDA) that it is safe and can be used as drug consumption [13].

There are many publications studying the efficacy of clove oil as fish anesthetic. They studied the induction and recovery ability of clove oil, as well as the behavior of European sea bass (*Dicentrarchus labrax*) [14], gilthead sea bream (*Sparus aurata*) [14], steelhead trout (*Oncorhynchus mykiss*) [15], Mekong giant catfish (*Pangasianodon gigas*) [11] and juvenile Angelfish (*Pterophyllum scalare*) [16]. The results showed that the dosage of clove oil was lower than commercial anesthetic for inducing fish to anesthesia as well as induction and recovery times were also shorter. Considering the effect criteria of complete anesthetic induction time within 3 minutes and recovery time within 5 minutes, the lowest effective dose in small juvenile angelfish was established at 100 ppm of clove oil whereas 140 ppm of MS-222 and 800 ppm of 2-phenoxyethanol were used [16]. Clove oil, MS-222 and 2-phenoxyethanol were able

to anesthetize in 2.31, 3.17 and 2.36 minutes and the recovery times was 3.31, 3.38 and 4.67 minutes, respectively. The optimal dosage of clove oil to anesthesia the European sea bass (weight of 32.5 g) and gilthead sea bream (weight of 41.9 g) was 30 ppm and 55 ppm, respectively, while that of 2-phenoxyethanol was 300 ppm and 450 ppm, respectively [14].

Moreover, clove oil was capable of reducing cortisol elevation in channel catfish (*Ictalurus punctatus*) (Fig. 2.2) [17], rainbow trout (*Oncorhynchus mykiss*) [18], common carp (*Cyprinus carpio*) [19], and Atlantic salmon (*Salmo salar* L.) [20]. Cortisol is the main substance to indicate the degree of stress in fish. As shown in Fig 2.2, MS-222 and quinaldine significantly increased the plasma cortisol concentrations comparing to clove oil and metomidate after 10-minute exposure. In addition, the level of cortisol when treated by clove oil did not change within 30 minutes.

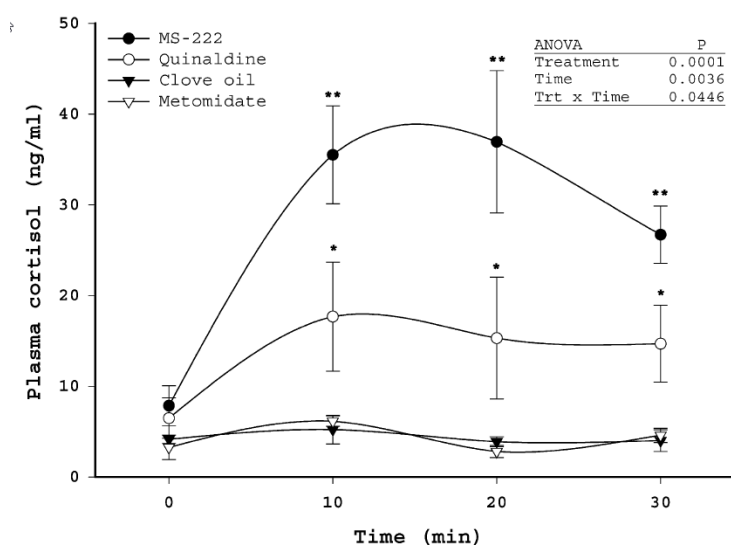


Figure 2.2 Plasma cortisol concentrations of channel catfish during 30-minute anesthetization with 100 ppm TMS, 30 ppm quinaldine, 100 ppm clove oil and 6 ppm metomidate [17]

Clove oil acts systemically when is absorbed through the gills and skin of fish [21]. Clove oil is highly lipophilic and therefore adheres and penetrates rapidly at the gill epithelium. Then, clove oil enters the blood circulation and is distributed throughout the body, such as the fat and brain. Clove oil decreases respiratory rates by inhibiting the respiratory center in the medulla oblongata and leading to reduced

oxygen uptake or conditions causing hypoxia (Fig. 2.3). Finally, the fish gradually lost consciousness.

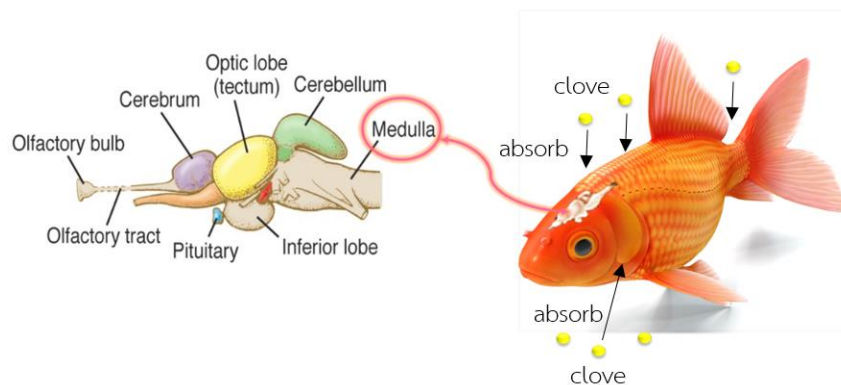


Figure 2.3 Mechanisms of anaesthesia

According to low water solubility of clove oil, ethanol is used to dissolve clove oil prior to pour in water with the 9:1 ratio of ethanol: clove oil. However, ethanol causes anxiety and irritation in fish [11].

2.3 Improvement solubility of clove oil

Encapsulation is the common technique to increase the water dispersion of hydrophobic compounds. The most common encapsulation systems are emulsions [22], liposomes [23] and polymersome [24]. Many studies reported the preparation of water-based clove oil. Clove oil emulsion for practical fish anesthesia composed of many chemicals such as ethanol, propylene glycol, β -hydroxy acid, polypropylene and ethylene diamine tetra-acetic acid [22]. The preparation of clove oil nano-emulsion was made by the ultrasonic emulsification method [25]. Tween 80 and Span 80 were used as surfactants. This emulsion contained 10 %wt of clove oil. The average droplet size of clove oil nanoparticles was 43 nm but the average droplets size of these particles increased to 100 nm after 6 months.

2.4 Edible film

Edible film has been received considerable attention in recent years to use as edible materials over synthetic films. This could contribute to the reduction of environmental pollution. Edible film is mostly used in both food and pharmaceutical industries such as food packaging, candy and drug delivery vehicle. Moreover, film can encapsulate active substances (antioxidants, antimicrobials, coloring, and flavors) for

applications in various fields. Encapsulated substances were good incorporated in the film matrix and be slowly released by evaporation of substance or the dissolution of film.

Film forming agents for edible film have been developed from abundant natural sources. The main film-forming materials are biopolymers, such as proteins, polysaccharides and lipids [26]. Proteins are macromolecules which consist of one or more long chains of amino acid residues. Protein films have conformational denaturation, electrostatic charges, and amphiphilic nature. Proteins can be easily modified to achieve desirable film properties by the use of heat denaturation, pressure, irradiation and chemical crosslinking. These treatments can ultimately control the physical and mechanical properties of edible protein film. Polysaccharides include starches, non-starch carbohydrates, gums, and fibers such as alginate, carboxymethyl cellulose, xanthan gum and pectin. Most carbohydrates are neutral, while some gums are charged negatively with very exceptional cases of positive charge. Due to the large numbers of hydroxyl groups or other hydrophilic moieties in the neutral carbohydrate structure, hydrogen bonds play the most significant role in film formation and property. Polysaccharide films have good water solubility property. Lipids are naturally occurring molecules that contain hydrocarbons such as acetylated monoglycerides, natural wax and surfactants [27]. It is soluble in nonpolar organic solvents. Thus, it can block transport of moisture. Lipid-based films are often supported on a polymer structure matrix, usually a polysaccharide, to provide mechanical strength. Biopolymers can be used alone or in the combination for preparation edible films.

Film can be prepared by several techniques such as dip coating, spray coating, spin coating, or solvent casting. Dip coating is a rapid and simple method. Film-forming polymers dissolve in solvent and then a desired coating material is dipped into the film-forming solution. After pick up material, solvent evaporates and the film-forming agent attaches on the surface of a material (Fig. 2.4).

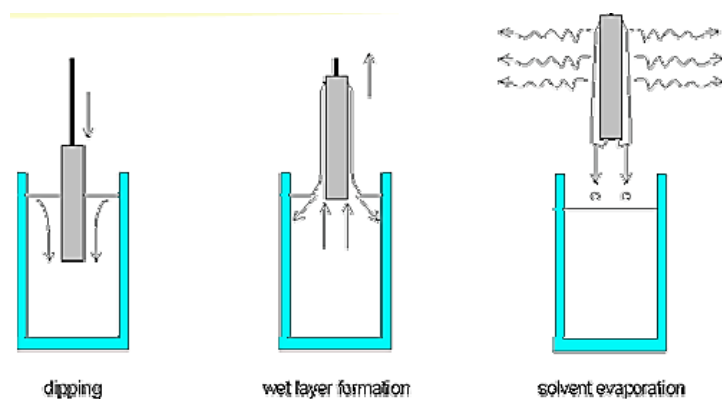


Figure 2.4 Dip coating process [28]

Spray coating is a method for coating thin film on the surface of the substrate [29]. It can use to coat on a wide variety types and shapes of the substrates. And this technique can control the thickness of film. Film-forming solution is directly sprayed on the surface of material, subsequently solvent dries and remove to induce the self-assembly of the smectic phase in the film. The mesomorphic structure is then stabilized by curing the matrix to form a robust coat of cured solvent.

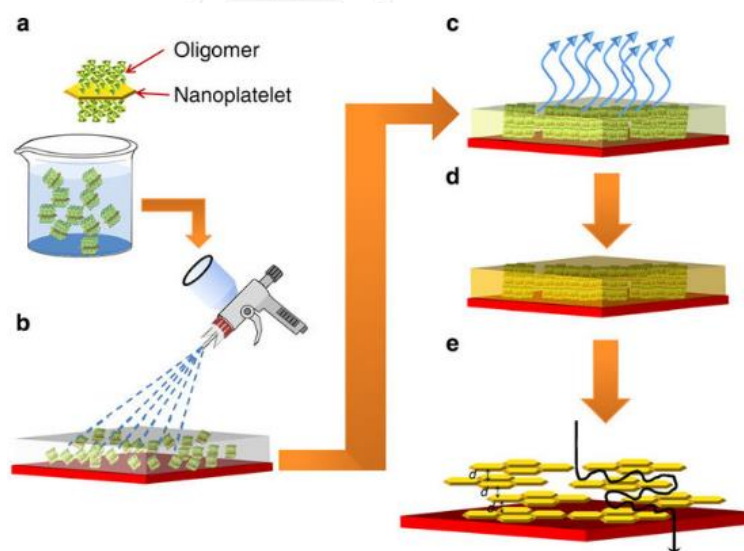


Figure 2.5 Spray coating

Spin coating is a method which the solvent in a dissolved or dispersed substance is removed by high speed spinning [30]. This process is widely used in the manufacture of integrated circuits optical mirrors, color television screens and magnetic disk. Centripetal acceleration will cause the resin to spread to, and eventually

off, the edge of the substrate leaving a thin film of resin on the surface. After that, the solvent removes to a certain extent in the spin-off stage and the viscosity of the film will increase. Film thickness and other properties depend on the nature of resin or the parameters chosen for the spin process.

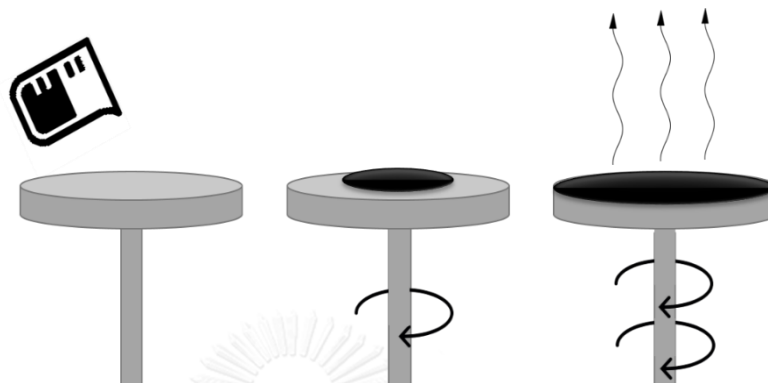


Figure 2.6 Spin coating process

The solvent casting is an easy method and more advantages including uniform thickness distribution, maximum optical purity and extremely low haze [31]. It customarily consists of casting the polymer–filler solution onto a mold and then evaporating the solvent without implementing further mechanical or thermal stress. After drying, film formed and can be peeled off from the mold.

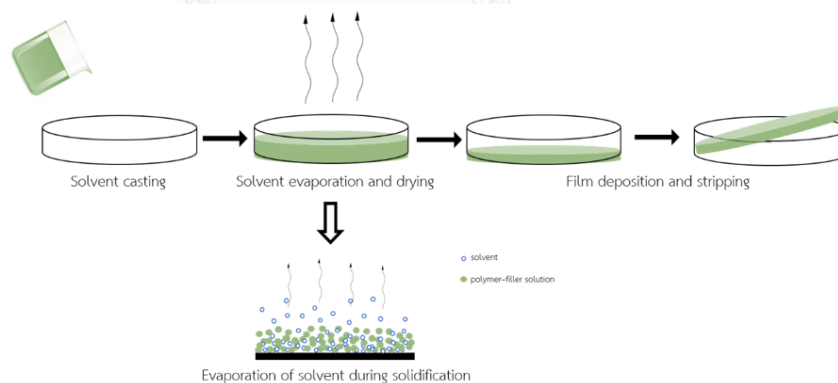


Figure 2.7 Solvent casting process

In this research, carboxymethyl cellulose and xanthan gum were chosen to use as film forming agents. Thus, we will give the information of these polysaccharides and their previous studies as film forming material.

Carboxymethyl cellulose (Fig. 2.5a) or CMC is a cellulose derivative with carboxymethyl groups ($-\text{CH}_2-\text{COOH}$) bound to some of the hydroxyl groups of the glucopyranose monomers [32]. CMC is a water-soluble polysaccharide at room

temperature. It is used as a viscosity modifier or thickener, and emulsion stabilizer in various food products including ice cream. In addition, CMC is used as a film forming polymer in many applications due to it has excellent film forming properties. Clove oil incorporated CMC film showed anti-microbial property toward pathogen bacteria (*Staphylococcus aureus*, *Bacillus cereus*, *Escherichia coli*, *Pseudomonas aeruginosa* and *Salmonella typhimurium*) [33]. It could be used for food packaging to retard of deterioration. The mixture of CMC and polyvinyl alcohol (PVOH) was used to encapsulate clove oil and used as an active packaging for ground chicken meat [34]. Polyvinyl alcohol (PVOH) enhanced mechanical property of film. Meat samples packed in this film had lower total viable counts and displayed a shelf life of 12 days, whereas, control samples spoiled within 4 days during refrigerated storage. Moringa leaf extract incorporated in the CMC and chitosan solution was coated on surface of avocado for enhancing quality and extending postharvest life [35]. The result showed that CMC reduced mass loss or moisture loss of avocado almost by 50% and reduced firmness loss resulted in improved fruit quality and shelf-life. Furthermore, fruit treated with moringa and CMC film had the highest concentration of C7 sugars, mannoheptulose, and perseitol, confirming their vital role in delaying fruit ripening process.

Xanthan gum (Fig. 2.5b) or XG is a natural polysaccharide and an important industrial biopolymer [36]. XG produces by the bacterium *Xanthomonas campestris* and be used in a wide variety of foods due to its compatibility with food ingredients and pseudoplastic rheological properties. It increases the emulsion stabilization and temperature stability of many food products. Moreover, XG has been used as an additive for edible film. A study reported the effect of XG on the physical and mechanical properties of gelatin-CMC film blends [37]. The addition of XG increased the thickness, moisture content and water vapour permeability of this film. Additionally, it reduced visible light transparency and increased thermal stability. Film contained XG showed lower tensile strength with diminished elongation at the break point, as well as higher puncture force and lower puncture deformation, indicating higher puncture resistance than comparable film without XG. A study reported the periodate oxidation of XG and its crosslinking effects on gelatin-based edible films [38]. The result showed that XG can drastically reduce mechanical properties and thermal

stability of gelatin films. On the other hand, oxidized XG was observed enhancement of water barrier properties, mechanical properties and thermal stability of gelatin due to the covalently linking between the two polymers.

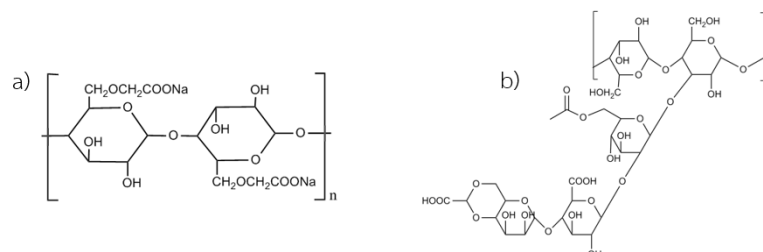


Figure 2.8 Chemical structures of a) carboxymethyl cellulose [32] and b) xanthan gum [38]

2.5 Alginate bead

Alginate is natural polysaccharides obtained from brown seaweed such as *Laminaria hyperborea*, *Laminaria digitata*, *Laminaria japonica*, *Ascophyllum nodosum*, and *Macrocystis pyrifera* [39]. It is a linear block co-polymer consisted of 1-4 linked β-D mannuronic acid (M) and α-L guluronic acid (G) residues. The blocks vary in size and alternating M and G segments as well as random blocks may also be present (Fig. 2.6). The ratio of M and G is depending on the weed source and growing conditions. Alginate has multiple properties such as film-forming [40], food gelling [41], stabilizing [42] and thickening properties [43].

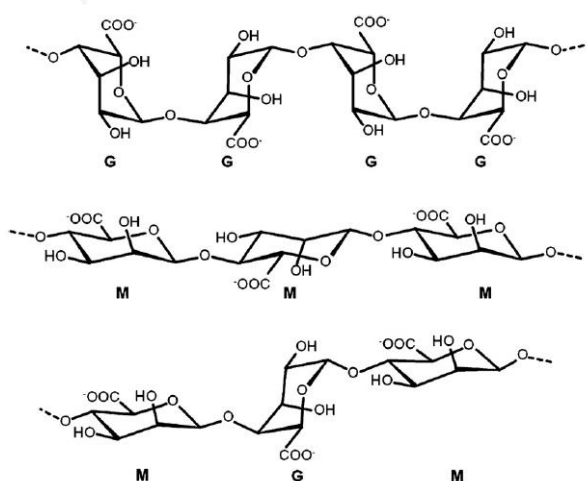


Figure 2.9 Chemical structures of G blocks, M blocks and MG blocks in alginate [39]

In addition, alginate can form bead by ionic cross-linking with divalent cations (Ca^{2+} , i.e.). The divalent cations are able to bind with G blocks of the alginate chains.

The one G blocks of polymer formed junctions with the other G blocks of adjoining polymer chain, the so call egg-box model (Fig. 2.7) [39]. Alginate beads are commonly used for many applications in pharmaceutical [44] and food industry [45] due to its general biocompatibility, non-toxicity, low cost, biodegradability and gel formation ability. Calcium alginate-CMC beads loaded anticancer drug 5-fluorouracil (5-FU) was prepared as a colon-specific oral drug vesicle [46]. CMC in the formulation retarded the release rate of 5-FU. In vitro release study, 5-FU released >90% from beads in the presence of colonic enzymes. Another study, essential oil- loaded alginate microspheres were prepared by spray alginate-oil emulsion into a collecting water bath containing calcium chloride solution [47]. Loading capacity and encapsulation efficiency of clove, thyme and cinnamon were 22-24% and 90-94%, respectively. This microsphere can reduce the rate of evaporation of the oil via microencapsulation and increase the antifungal activity of essential oils. There was a study encapsulating polyphenols from *Clitoria ternatea* petal flower extract in alginate bead [48]. The encapsulation efficiency was $84.83 \pm 0.40\%$ and alginate bead improved the thermal stability of flower extract at $188\text{ }^{\circ}\text{C}$.

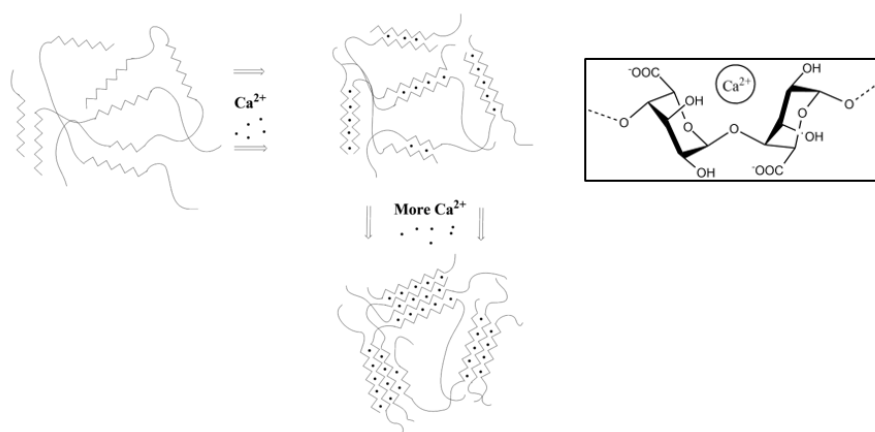


Figure 2.10 Binding to calcium ions by G-block in alginate and Egg-box model structure of an alginate gel formation [49]

CHAPTER III

EXPERIMENTAL

3.1 Chemicals and materials

Clove oil (CO) extracted by steam distillation was obtained from Thai-China Flavours and Fragrances Industry Co., Ltd. (Thailand). Carboxymethyl cellulose (CMC), sodium alginate (SA) and xanthan gum (XG) was purchased from Union Chemical 1986 Co., Ltd. (Thailand). Calcium chloride (CaCl_2) was purchased from Sigma (USA). Organic solvents were AR grade. The marine salt purchased from Q-SEA®.

3.2 Chemical stability of clove oil

Clove oil was kept 2 systems for 1 year. Closed system was storage in opaque bottle in refrigerator. Open system was storage in clear bottle at room temperatures. 20 μL of clove oil in both systems were dissolved in CDCl_3 and were evaluated the main composition by ^1H NMR analysis using a Brüker Oxford instrument.

3.3 Preparation of film

The different ratio of film-forming polymers as shown in Table 3.1 was used to prepared clove oil film. The film-forming solution was prepared by dissolving polymers in distilled water under continuous magnetic stirring at 70°C to achieve a clear solution. Then clove oil (2% w/v) was added in the film-forming solution and blended by homogenizer (IKAT25-Digital Ultra Turrax, Staufen, Germany) 4000 rpm at room temperature for 5 minutes. The 20 g of mixture was poured in a circular stainless plate with 8.5 cm diameter and dried in the oven at 60°C for 12 hours. The dried film was peeled off and stored in the desiccators at 35% humidity until evaluation. The ratio of film-forming polymers which gave the highest entrapment efficiency and loading capacity percentages was consequently studied by vary the different concentrations

of clove oil; 2, 3, 4, 5 and 6% (w/v). The proper concentration of clove oil which gave the highest entrapment efficiency and loading capacity percentages was further characterized the physical properties and shelf-life stability. The control film was prepared without clove oil.

The percentages of encapsulation efficiency (%EE) and loading capacity (%LC) were calculated using equations (1) and (2), respectively.

$$\%EE = \frac{\text{Weight of clove oil in film}}{\text{Initial weight of clove oil}} \times 100 \quad (1)$$

$$\%LC = \frac{\text{Weight of clove oil in film}}{\text{Weight of clove oil film}} \times 100 \quad (2)$$

Table 3.1 Compositions of film-forming polymers used for preparing clove oil film

Sample	CMC (%)	XG (%)	CO (%)
C ¹ X ¹	1	1	2
C ¹ X ^{0.1}	1	0.1	2
C ¹ X ^{0.2}	1	0.2	2
C ¹ X ^{0.3}	1	0.3	2
C ¹ X ^{0.4}	1	0.4	2
C ¹ X ^{0.5}	1	0.5	2
C ¹ X ^{0.6}	1	0.6	2

3.4 Physical properties of films

3.4.1 Thickness

Film thickness was determined with a digital electronic vernier caliper micrometer (Mituto, Tokyo, Japan) with a sensitivity of 0.01 mm. Each film sheet was measured at different points at least seven random locations and results reported as mean and standard deviation.

3.4.2 Water solubility

To prepare 20 and 50 ppm of clove oil in the water, approximately 6.7 and 16.7 mg of CO films were used to study the water solubility of CO film in 100 mL of the distill water and sea water.

Samples were weighed to gain the initial weight (W_i). Then, samples were immersed in 100 mL of distill water with mild stirring at room temperature for 5 minutes. After filtration, the undissolved samples were dried at 100 °C for 24 h to obtain the dry matter weight (W_f). The water solubility of film was determined by the following expression:

$$\% \text{water solubility} = \left[\frac{W_i - W_f}{W_i} \right] \times 100 \quad (3)$$

Where W_i is the initial weight of the dry matter and W_f is the dry matter weight of the dispersion process after 5 minutes.

The film was also studied the solubility in seawater using the same procedure as in distilled water.

3.4.3 Color

The color of samples includes " L^* " value, that indicates the lightness [black ($L^* = 0$) and white ($L^* = 100$)], " a^* " value that indicates redness–greenness [total red ($a^* = 100$) and total green ($a^* = -100$)], and " b^* " value that indicates yellowness–blueness [total yellow ($b^* = 100$) and total blue ($b^* = -100$)] were measured by the Minolta Chroma Meter CR-400 (Minolta Co., Ltd, Japan). The measurements were taken on white standard backgrounds ($L = 90.45$, $a = 2.61$ and $b = -5.00$). Total color difference (ΔE) was calculated using the equations 3.

$$\Delta E = \sqrt{(L^* - L)^2 + (a^* - a)^2 + (b^* - b)^2} \quad (4)$$

Where L^* , a^* , and b^* are the color parameter values of the film and L , a , and b are the color parameter values of the standard.

3.4.4 Moisture content

Moisture content of film was determined by the loss of weight of film after drying at 105 °C for 24 h. The weight of film before and after drying was calculated for the moisture content using the following equation;

$$\% \text{moisture content} = \left[\frac{W_b - W_a}{W_b} \right] \times 100 \quad (4)$$

Where W_b and W_a were weights before and after drying

3.4.5 Scanning electron microscopy (SEM)

The surface and cross-section texture of film were examined by scanning electron microscope (SEM) (JSM-6480LV, JEOL, Japan). The samples were mounted on the metal stub, using double sided adhesive tape, gold coated under vacuum and the images were taken at 15 kV.

3.4.6 Thermal gravimetric analysis (TGA)

The thermogravimetric characteristic of CMC, XG, control film and clove oil film was measured by TGA (SDTA851e, Mettler Toledo, Columbus, USA). This technique was used to determine the onset temperature of overall thermal degradation (Td) of samples. The samples were heated from 30 to 600°C at the rate of 10 °C/min with nitrogen gas purged at 30 ml/min.

3.4.7 Fourier transformed infrared (FTIR) spectroscopy

Infrared (IR) spectrum of samples were recorded with a Nicolet 6700 FT-IR spectrophotometer (Thermo Electron Scientific, Madison, WI) spectrometer using the attenuated total reflection (ATR) method. Samples were scanned between 600 cm^{-1} and 4000 cm^{-1}

3.5 Solubility of clove oil

Pure and complexed clove oil at 1000, 1500, 2000, 2500, 3000, 3500, 4000, 5000 and 6000 ppm were diluted in distilled water and seawater with 10:90 (v/v)

proportion. A sample solution was subjected to centrifugal separation at 4000 rpm to allow particles to sediment. The sample to the top of the gradient the tube was analyzed for clove oil content using UV-visible spectrophotometer at 280 nm. The highest solubility of clove oil in distilled water and seawater were obtained at the first maximum absorbance.

The seawater was prepared by measuring 3.7 g of marine salt (Na^+ 42.2, K^+ 0.9, Mg^{2+} 4.8, Ca^{2+} 0.8, Sr^{2+} 0.01, Cl^- 48.2, SO_4^{2-} 2.6 and Br^- 0.74 mmole/kg) dissolve in 100 mL of distilled water.

3.6 Preparation of beads

The different ratio of SA, CMC and XG (Table 3.2) was used to prepared clove oil beads. Those polymers were dissolved in distilled water under continuous magnetic stirring at 70°C to achieve a clear solution. After the solution cool down, 2% (w/v) of clove oil was added and homogenized 4000 rpm at room temperature for 5 minutes. Then the mixture was extruded via a needle (2 mm diameter) into 2% calcium chloride solution with gentle agitation at room temperature for 15 minutes. Then beads were taken out and washed with distilled water three times. Beads were allowed to dry at 40°C for 24 hours. The dried beads were stored in a desiccator at 35% humidity until evaluation. The control bead was prepared without clove oil.

Table 3.2 Compositions of mixture for preparing clove oil beads

Sample	CMC (%)	XG (%)	SA (%)
A ¹	-	-	1
A ²	-	-	2
C ¹ A ¹	1	-	1
X ¹ A ¹	-	1	1
C ^{0.5} X ^{0.5} A ¹	0.5	0.5	1
C ¹ X ¹ A ¹	1	1	1

The ratio of polymer which gave the highest swelling rate was consequently characterized the physical properties and shelf-life stability. Shelf-life stability was studied by keeping clove oil beads in 2 conditions; vacuum and non-vacuum sealed foil bags. Beads were then characterized properties at 0, 15, 30, 60, 90 and 120 days of the storage period.

The percentages of encapsulation efficiency (%EE) and loading capacity (%LC) were calculated using equations (5) and (6), respectively

$$\%EE = \frac{\text{Weight of clove oil in film}}{\text{Initial weight of clove oil}} \times 100 \quad (5)$$

$$\%LC = \frac{\text{Weight of clove oil in beads}}{\text{Weight of clove oil beads}} \times 100 \quad (6)$$

3.7 Swelling study

Seven test tubes with samples were prepared. Each test tube contained dry beads about 0.0160 g and 2 mL of distilled water. At the interval times 15, 30, 45, 60, 75, 90, 105, 120, 135, 150, 165 and 180 minute, the beads were taken out, suddenly wiped the surface by tissue paper and weighed. The fractional weight change was transformed to a percentage using the following empirical relationship

$$\% \text{weight change} = \frac{\text{Final weight} - \text{Initial weight}}{\text{Initial weight}} \times 100 \quad (7)$$

The beads were also studied the swelling rate in seawater using the same procedure as in distilled water.

3.8 Release study

The release behavior of clove oil from beads was carried out in distilled water at room temperature. Clove oil beads (~ 0.1200 g) were immersed in 100 mL of distilled water. At 2, 4, 6, 8, 10, 12, 24 hours intervals, 250 μ L of medium was collected periodically and replaced with fresh distilled water. The collected medium was analyzed for clove oil content using UV- visible spectrophotometer at 280 nm. Cumulative percentage of clove oil release was calculated using the equation below:

$$\% \text{release clove oil} = \frac{\text{clove oil released}}{\text{total encapsulated clove oil}} \times 100 \quad (8)$$

The clove oil beads were also studied the release behavior in the simulated seawater using the same procedure as in distilled water.

3.9 Physical properties of beads

3.9.1 Size

Size of bead was determined with a digital electronic vernier caliper micrometer (Mituto, Tokyo, Japan) with a sensitivity of 0.01 mm. Each film sheet was measured at different points at least seven random locations and results reported as mean and standard deviation.

3.9.2 Moisture content

Moisture content of beads was determined by the loss of weight of the beads after drying at 105 °C for 24 **hours**. The weight of beads before and after drying was calculated for the moisture content

$$\% \text{moisture content} = \left[\frac{W_0 - W_1}{W_0} \right] \times 100 \quad (9)$$

Where W_0 and W_1 were weights before and after drying

3.9.3 Scanning electron microscopy (SEM)

The surface and cross-section texture of beads was examined by scanning electron microscope (SEM) (JSM-6480LV, JEOL, Japan). The samples were mounted on the metal stub, using double sided adhesive tape, gold coated under vacuum and the images were taken at 15 kV.

3.9.4 Fourier transformed infrared (FTIR) spectroscopy

Infrared (IR) spectra of beads was recorded with a Nicolet 6700 FT-IR spectrophotometer (Thermo Electron Scientific, Madison, WI) spectrometer using the attenuated total reflection (ATR) method. Samples were scanned between 600 cm^{-1} and 4000 cm^{-1}

3.10 Stability study

Shelf-life stability of clove oil film and bead was studied. The samples were packed in foil bags with and without vacuum at $40\text{ }^{\circ}\text{C}$. Samples were characterized their thickness (or size), color and %LC at 15, 30, 60, 90 and 120 days of the storage period. Moisture content was tested at 60 and 120 days of the storage period. The FTIR spectrum and SEM images of samples were evaluated at 60 and 120 days. Solubility of clove oil film was tested at 60 and 120 days of the storage period and TGA of film was done at 60 and 120 days of the storage period.

CHAPTER IV

RESULT AND DISCUSSION

4.1. Chemical stability of clove oil

The ^1H NMR spectrum of clove oil between closed and open systems were presented in Fig. 4.1. The spectrum showed the signals of eugenol which is the major component of clove oil. The result indicated that the majority component is chemically stable.

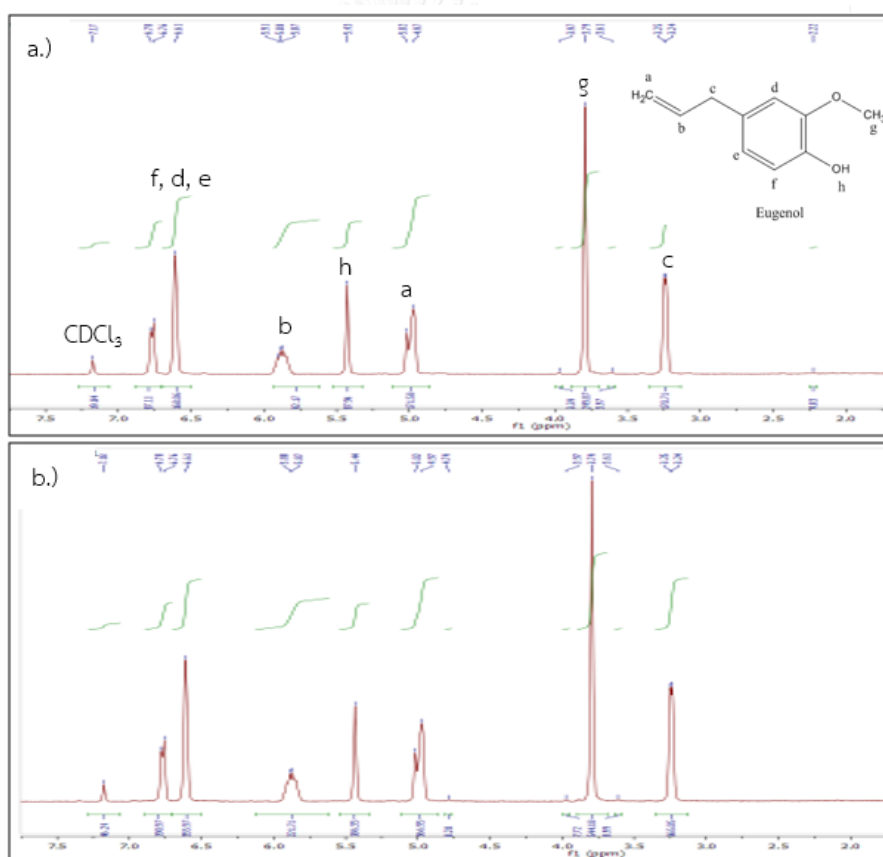


Figure 4.1 The NMR spectrum of clove oil in a) closed system and b) open system

4.2 Entrapment efficiency (EE) and loading capacity (LC) of clove oil films

The clove oil films (CO film) were firstly study the influence of the XG amount toward EE and LC. To evaluate the amount of the CO incorporated in the films, the major component which is eugenol was determined by gas chromatography (GC)

spectrometry. The results shown in Table 4.1 indicated that the $C^1X^{0.4}$ had the highest EE and LC. Thus, it was selected for next study. However, this film formula gave quite thin film and CO would be entrapped in low amount. Therefore, the amount of CMC and XG was increased twice as 2% w/v of CMC and 0.8% w/v of XG to fabricate $C^2X^{0.8}$ film. The various concentrations of CO in $C^2X^{0.8}$ film were studied and the results were shown in Table 4.2. Consideration LC percentage, it was found that 4% CO gave the highest EE percentage. But according to the oily surface of 3% and 4% of CO films, the film composition of 2% CMC, 0.8% w XG and 2% w CO was chosen for further study.

Table 4.1 The LC and EE percentages of the CO films by varying the XG concentrations

Sample	%LC	%EE
$C^1X^{0.1}$	21.1 ± 0.4 ^a	29.9 ± 1.3 ^a
$C^1X^{0.2}$	22.6 ± 0.4 ^{ab}	31.2 ± 0.7 ^a
$C^1X^{0.3}$	22.6 ± 0.8 ^{ab}	34.7 ± 1.6 ^a
$C^1X^{0.4}$	25.8 ± 1.5 ^b	49.6 ± 3.2 ^b
$C^1X^{0.5}$	23.0 ± 1.9 ^{ab}	37.9 ± 3.1 ^a
$C^1X^{0.6}$	21.0 ± 2.8 ^a	40.4 ± 8.9 ^{ab}
C^1X^1	21.2 ± 1.8 ^a	38.1 ± 2.3 ^a

^{a, b} Different superscripts within a column indicate significant differences ($p < 0.05$)

Table 4.2 The LC and EE percentages of the $C^2X^{0.8}$ film by varying the CO concentration

Clove oil (%)	%LC	%EE
2	32.7 ± 0.5 ^c	53.5 ± 0.8 ^c
3	44.8 ± 1.7 ^b	60.7 ± 2.3 ^b
4	62.6 ± 1.9 ^a	72.0 ± 2.1 ^a
5	58.2 ± 1.9 ^a	54.1 ± 1.7 ^a

^{a-c} Different superscripts within a column indicate significant differences ($p < 0.05$)

4.3 Characterization of CO film

4.3.1 Appearance, color and thickness

The control film was transparent and colorless whereas CO film had slight yellowish color due to the color of CO (Fig.4.2). The color of film was detected using Hunter L*, a*, b* scale. The L* value of the control film was 88.06 ± 2.13 and that of the CO film was 85.53 ± 0.47 . The high L* value indicated that the control film was more transparent than the CO film. The yellowness +b* value of CO film was 4.34 ± 0.29 while that of control film was 0.33 ± 0.59 . And the greenness +a* value of CO film (0.46 ± 0.05) was slightly higher than that of the control film (0.13 ± 0.02). The average thickness of control and CO film was 0.08 ± 0.01 and 0.12 ± 0.02 mm, respectively, measured by a digital micrometer. The incorporation of CO into the film forming matrix increase the thickness of film.



Figure 4.2 a) control film and b) CO film

4.3.2 Water solubility and moisture content

The control and CO film was dissolved in water and seawater. The concentration of CO in film at 20 and 50 ppm was prepared by weight measurement the CO film 6.7 and 16.7 mg. The control film was prepared at the same weight. Then films were dissolved in 100 mL of distilled water and seawater. The result showed that the both concentration (Fig.4.3) showed the same approach. The control film had the solubility higher than CO film due to hydrophobic of clove oil. The solubility of film in seawater was slower than that in water because to increase the ionic strength of medium. If the film is cut into small pieces, it will increase the solubility.

The moisture content of control and CO films was 16 ± 3.4 and $10 \pm 4.1\%$, respectively. Incorporation of CO into the CMC and XG matrix decrease the moisture content percentage of the film. From previous research found that addition essential oil in film forming led to decrease the moisture content. Klangmuang, P. et al. [50] and Qiumin, M. et al. [51] have reported similar results of adding oil to film composition.

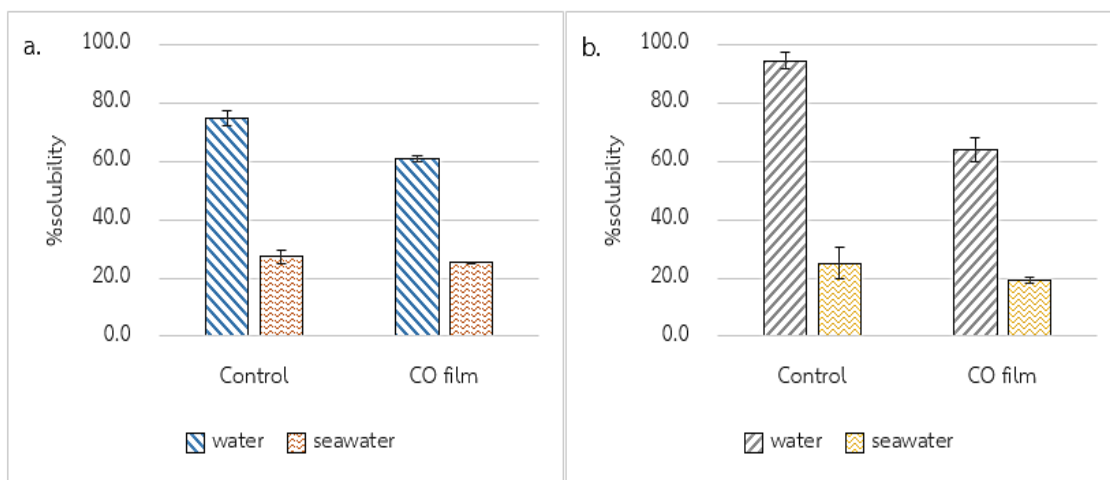


Figure 4.3 The solubility of control and CO film at a) 20 ppm and b) 50 ppm of CO in film

4.3.3 Microstructure of films

The SEM images of the control and CO films were shown in the Fig. 4.4. The surface of the control film was smoother than that of the CO films. The cross-section micrograph of the CO film showed the different sizes of oil droplets dispersed in the polymer matrix while control film had no any porous. This dispersion caused by the homogenize speed and were stabilized by the hydrophilic property of polymer chain to inhibit the agglomerate of CO droplets.

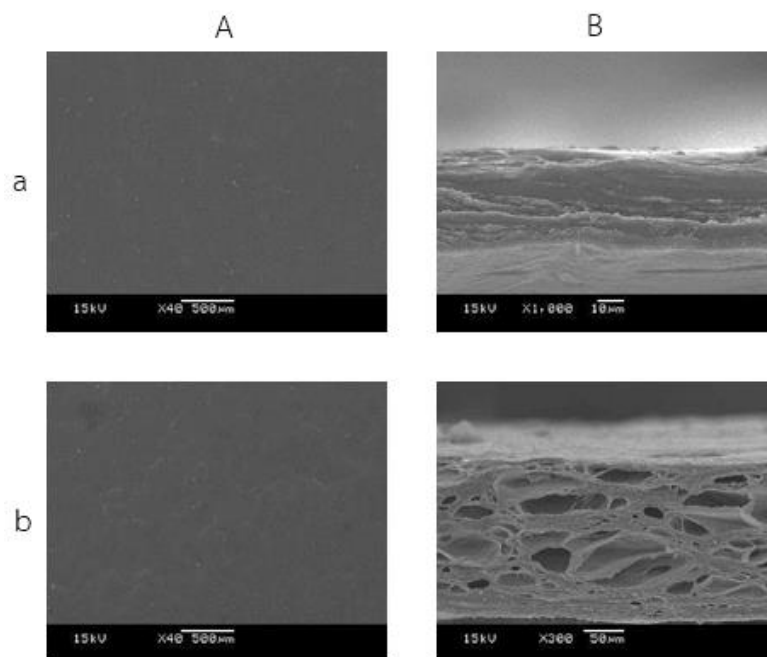


Figure 4.4 SEM micrographs of the surfaces (left column, A) and cross-sections (right column, B) of the a) control film and b) CO film.

4.3.4 Fourier-transform infrared (FTIR) spectroscopy

FTIR spectra of CO, control and clove oil films shown in Fig. 4.5 showed similar peaks of the broad band of O-H stretching of alcohol at 3327 cm^{-1} , C-H stretching peak of aromatic at 2917 cm^{-1} , The C=O stretching peak of carbonyl at 1589 cm^{-1} , the C-O-C stretching peaks of ether at $1234\text{-}1325\text{ cm}^{-1}$, the adsorption peak of C-C stretching peak of aromatic at 1408 cm^{-1} and the adsorption peak of C-O stretching of alcohol at 1025 cm^{-1} . The presence of CO in film confirmed by the appearance of the C=C stretching peak at 1514 cm^{-1} of eugenol.

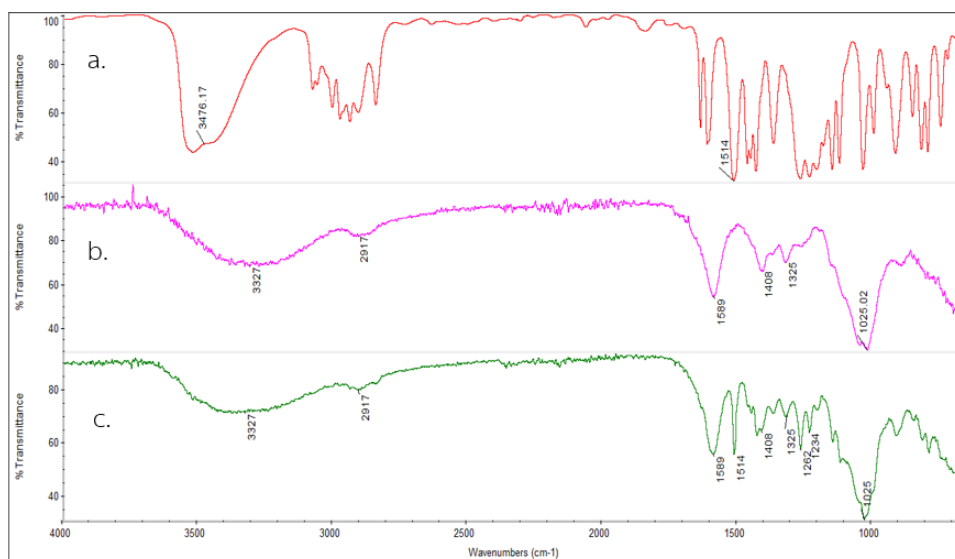


Figure 4.5 FTIR spectra of a) CO b) control film and c) CO film

4.3.5 Thermal stability

Thermogravimetric analysis (TGA and DTG) was performed to evaluate the thermal stability of the film. TGA and DTG curves for all prepared films indicated a similar thermal behavior with slight difference which related to the composition of the samples. The mass loss evolution with temperature of CMC powder, XG powder, control film and CO film were shown in Fig. 4.6. The first step of thermal degradation corresponded to the loss of water. The degradation temperature of CMC and XG (Fig. 4.6a and 4.6b) was found at 306 and 284°C, respectively. The control film (Fig. 4.6c) had a degradation temperature in a combination manner of CMC and XG at 286 °C. Fig. 4.6d showed degradation temperature of the CO film at 267 °C. However, mass loss evolution with temperature of CO film increased compared to control film which indicated the presence of CO in film.

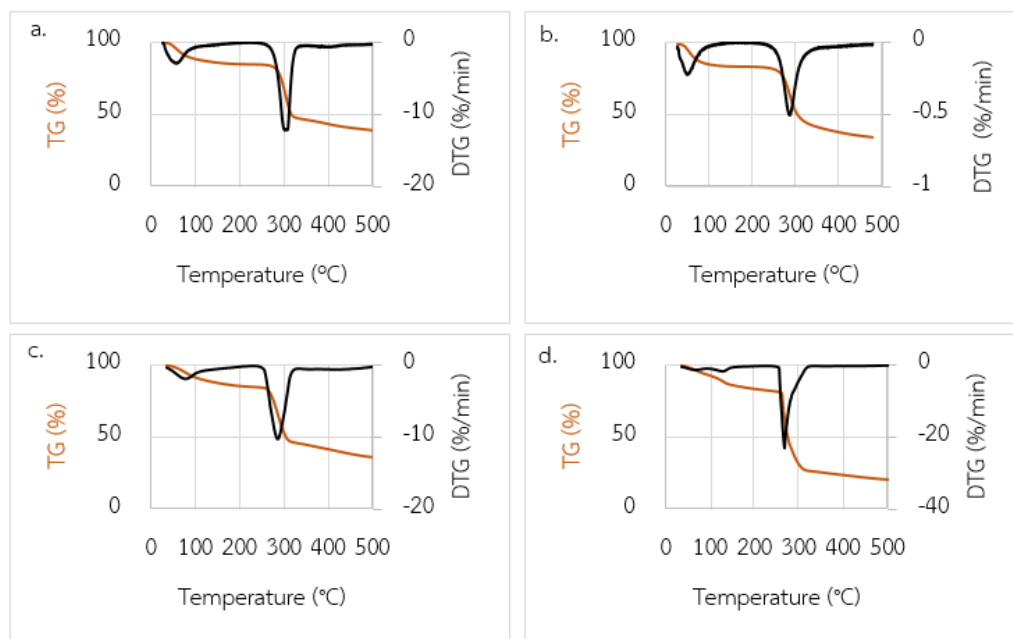


Figure 4.6 TGA curves and DTG thermograms of a) CMC, b) XG, c) control film and d) CO film

4.4 Water solubility of clove oil and clove oil in film

Fig. 4.7 showed the solubility of CO in water and sea water. CO is able to dissolve in the sea water less than in the water. The CO reached the maximum solubility around at 30 ppm whereas CO in films extended solubility higher than 60 ppm.

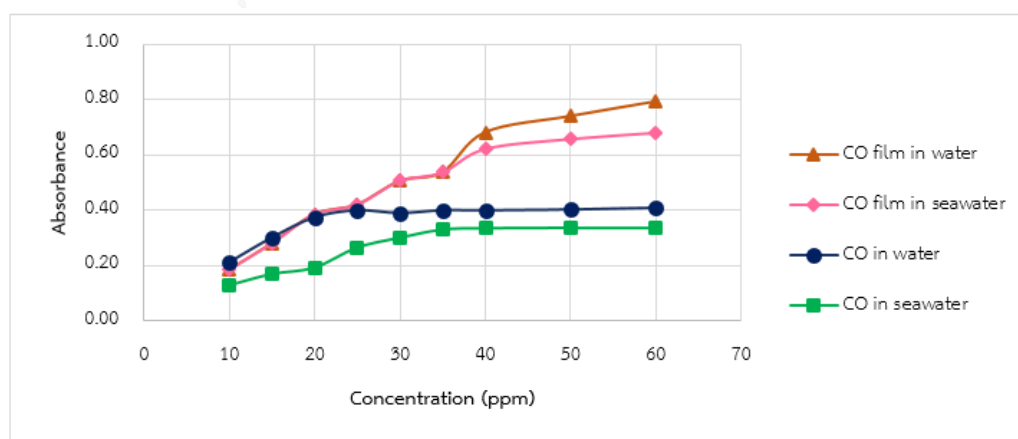


Figure 4.7 The solubility of CO and CO film in water and seawater

4.5 Preparation of beads

Six types of alginate beads were prepared and the dried beads were then studied the swelling rate in the distill water. As shown in Fig. 4.8, the $A^1C^1X^1$ and $A^1C^{0.5}X^{0.5}$ beads exhibited the dynamic weight change faster than other beads. CMC and XG components in the alginate obstructed the ionic cross-linking between Ca^{2+} and the carboxylate group of the alginate chains. This resulted in the easier penetration of water molecule into the inner matrix of alginate. However, the bead shape of $A^1C^{0.5}X^{0.5}$ was more spherical than that of $A^1C^1X^1$. Thus, $A^1C^{0.5}X^{0.5}$ beads were used for further study in this research. Swelling of the dry beads is mainly attributed to the hydration of the hydrophilic groups of alginate. In this case, free water penetrates inside the beads in order to fill the inert pores among the polymer chains, contributing to a greater swelling degree. The $A^1C^{0.5}X^{0.5}$ beads was incorporated with 2% CO (CO beads) which gave the LC and EE percentage about 8.0 ± 0.4 and $11.9 \pm 0.6\%$, respectively.

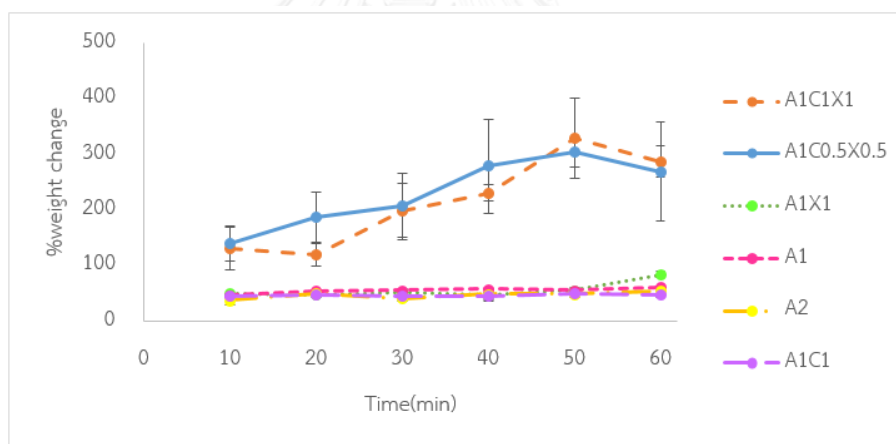


Figure 4.8 Swelling profiles of the six types of alginate beads in water at the interval times

4.5.1 Swelling and releasing study

The CO beads were evaluated the dynamic weight change in water and seawater for 180 min. The result showed in Fig. 4.7. The CO beads can swell 230 ± 12 and $296 \pm 11\%$ in the distilled water and the seawater, respectively. The beads swell gradually in both systems until 180 min as 507 ± 8 and $638 \pm 33\%$ in the water and the seawater, respectively. Over all, the CO beads swelled in the seawater faster than in the water with statistically significant ($p < 0.05$). This might due to the presence of

many cations such as Na^+ and K^+ in seawater undergo ion-exchange process with Ca^{2+} ions.

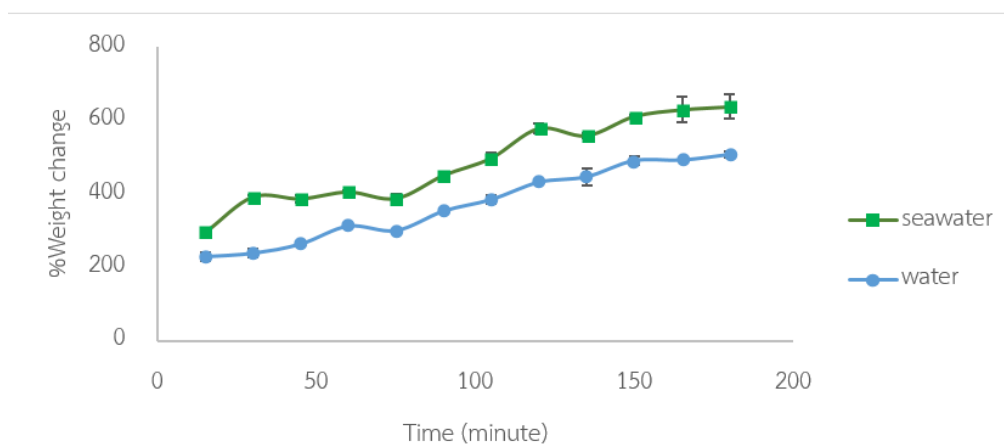


Figure 4.9 Swelling profiles of the CO beads in water and seawater for 180 minutes

Release of clove oil in bead caused by the bead swelling and water penetration inside the beads. The result shown in the Fig. 4.8 indicated that clove oil released from the CO beads in the water faster than in the seawater with statistically significant ($p < 0.05$). However, CO cannot 100% releasing within 180 min. In this study, we have expected that CO released from CO bead in the form of encapsulated particles. CO was entrapped in the matrix of CMC and XG in the same way as the CO film. In releasing study, there was no phase separation between CO and release medium which can confirm our expectation. CO beads swelled faster but CO particles released slower in the seawater. It was caused by increase the ionic strength of medium.

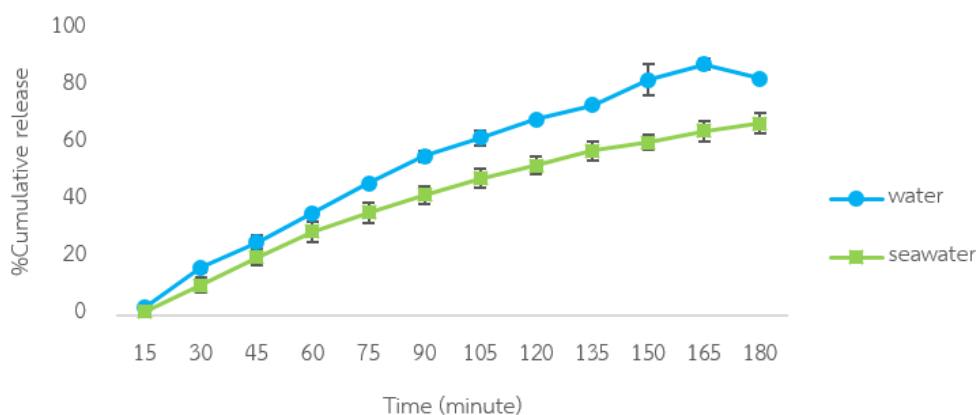


Figure 4.10 Cumulative release of CO in water and seawater for 180 minutes

4.5.2 Morphology of the beads

The control beads were flat with the average diameter of 2.37 ± 0.07 mm whereas the CO beads were irregularly flat and not spherical with the average diameter of 1.56 ± 0.03 mm as shown in Fig. 4.11. The control beads were colorless and the CO beads were yellowish due to the color of CO. Moisture content percentage of CO beads ($13 \pm 0.8\%$) was lower than control beads ($22 \pm 0.5\%$). CO droplets were dispersed in the polymer matrix by the homogenize speed and stabilized by the hydrophilic property of polymer chain to inhibit the agglomerate of CO droplets that showed in Fig.4.12.

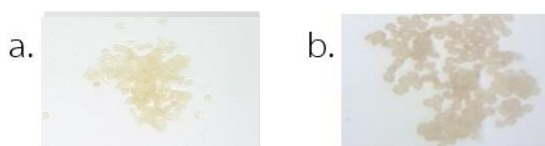


Figure 4.11 Photos of a) control beads and b) CO beads by a digital camera

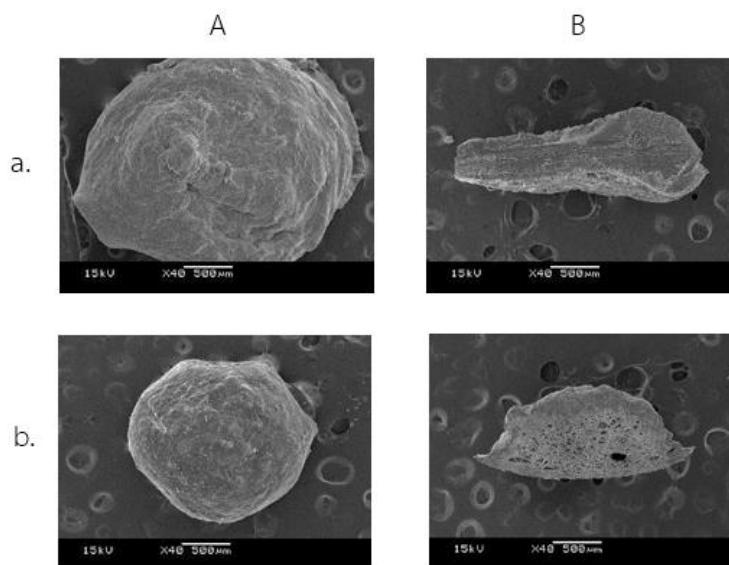


Figure 4.12 SEM micrographs of the surfaces (left, A) and cross-sections (right, B) of the a) control bead and b) CO bead.

4.5.3 Fourier-transform infrared (FTIR) spectroscopy

FTIR spectra of CO, control beads and CO beads shown in Fig. 4.13 showed similar peaks of the broad band of O-H stretching of alcohol at 3342 cm^{-1} , the C-H stretching peak of aromatic at 2897 cm^{-1} , The C=O stretching peak of carbonyl at 1589 cm^{-1} , the C-O-C stretching peaks of ether at $1234\text{-}1325\text{ cm}^{-1}$, the adsorption peak of C-

C stretching peak of aromatic at 1425 cm^{-1} and the adsorption peak of C-O stretching of alcohol at 1025 cm^{-1} . The presence of CO in film confirmed by the appearance of the C=C stretching peak at 1514 cm^{-1} of eugenol.

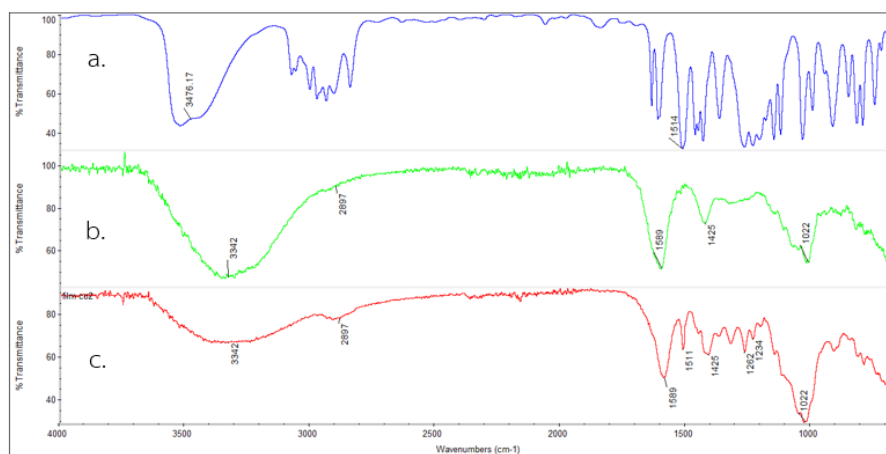



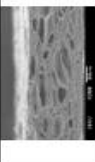
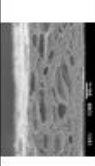
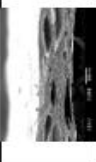


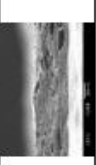
Figure 4.13 FTIR spectrum of a) CO, b) control bead and c) CO bead.

4.6 Shelf-life stability of CO film

4.6.1 Appearance, color and thickness

The photograph images of the stored CO films were summarized in Table 4.3. The result showed that The color of CO film was gradually yellowed when were stored for 120 days due to the color change of clove oil which corresponds to b^* values in Fig. 4.14. The more positive b^* value means more yellowish color. The L^* value of CO film in non-vacuum conditions was less than in vacuum conditions show that CO film in non-vacuum conditions was more opacity. The thickness of all the vacuum and non-vacuum CO films were not significantly different ($p < 0.05$) after 120 days which showed in Table 4.3.

Table 4.3 Appearance and thickness of CO film in vacuum and non-vacuum conditions

Day	Vacuum				Non-vacuum			
	Appearance	Size (mm)	Surfaces	Cross-sections	Appearance	Size (mm)	Surfaces	Cross-sections
0	CHULA	0.12 ± 0.02			CHULA	0.12 ± 0.01		
15	CHULA	0.11 ± 0.01	-	-	CHULA	0.12 ± 0.01	-	-
30	CHULA	0.12 ± 0.01	-	-	CHULA	0.13 ± 0.01	-	-
60	CHULA	0.13 ± 0.01			CHULA	0.13 ± 0.01		
90	CHULA	0.13 ± 0.01	-	-	CHULA	0.13 ± 0.01	-	-
120	CHULA	0.13 ± 0.01			CHULA	0.13 ± 0.01		

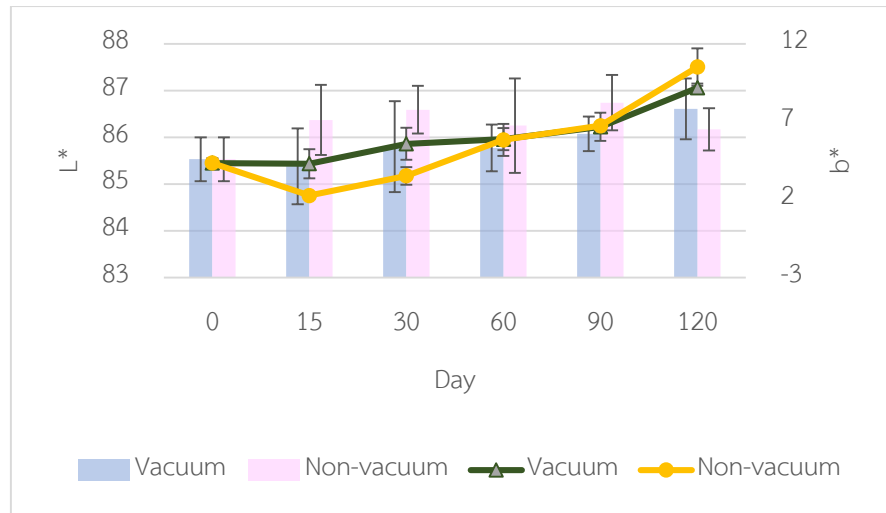


Figure 4.14 Color of CO film in vacuum and non-vacuum conditions

4.6.2 LC percentage and SEM analysis CO film in vacuum and non-vacuum conditions.

The LC percentages of CO film for 120 days showed in Fig.4.15. The CO amount in film gradually decreased within 60 days and after that the amount keep unchanging. The LC percentages of vacuum and non-vacuum storage were not significantly different ($p < 0.05$). The decreasing of CO amount correlated to the lessening of CO droplet size shown in the SEM images (Table 4.3).

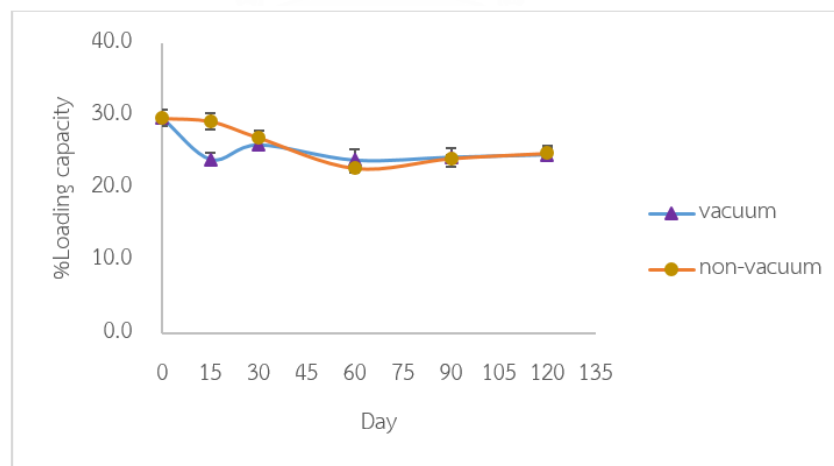


Figure 4.15 The %LC of CO film in vacuum and non-vacuum conditions

4.6.3 Solubility and moisture content

The water and seawater solubility of the vacuum and the non-vacuum CO films within 120 days were shown in Fig. 4.16 The water and seawater solubility of films

gradually decreased during the storage by a function of time but not significantly different between the vacuum and the non-vacuum CO films. Moreover, the lessening of the water solubility of the CO films might be caused by the collapse of network since polymer chains mobility is restricted by the extension of the intra- and inter molecular hydrogen bonds network between the cellulose chains. The moisture of CO film after 120 days (Fig. 4.17) was not significant difference ($p < 0.05$)

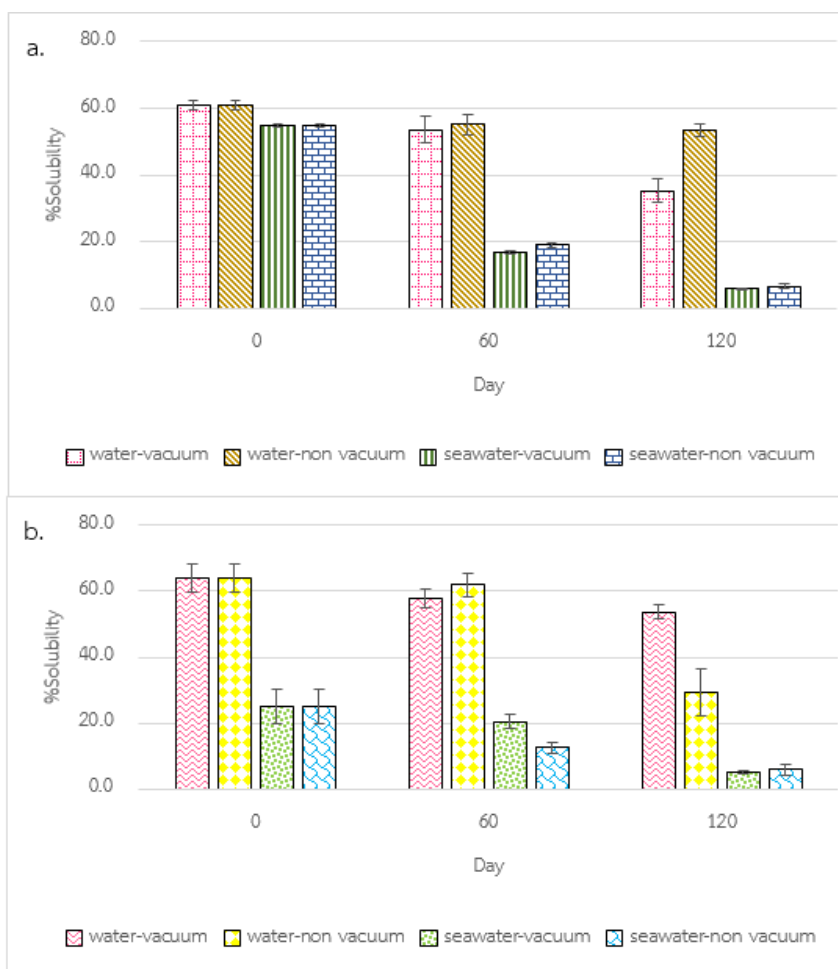


Figure 4.16 The water and seawater solubility of CO film at a) 20 and b) 50 ppm of CO within film in vacuum and non-vacuum condition

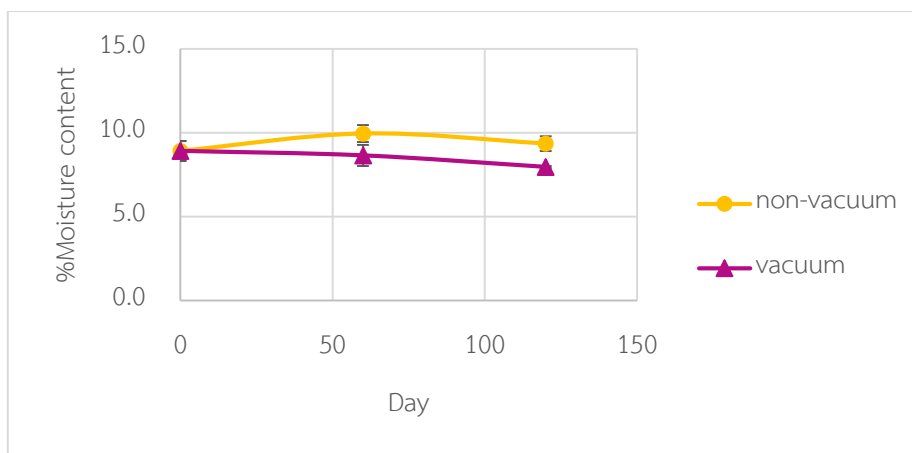


Figure 4.17 The moisture content of CO film in vacuum and non-vacuum condition

4.6.4 Thermal stability

The TGA (Fig. 4.18a) and DTG (Fig. 4.18b) thermograms of CO films after storage at 0, 60 and 120 days in vacuum and non-vacuum condition are shown. The thermal degradation events of CO films were observed in the 244–314 °C range. The mass loss slightly decreased and there was no difference between both storage condition.

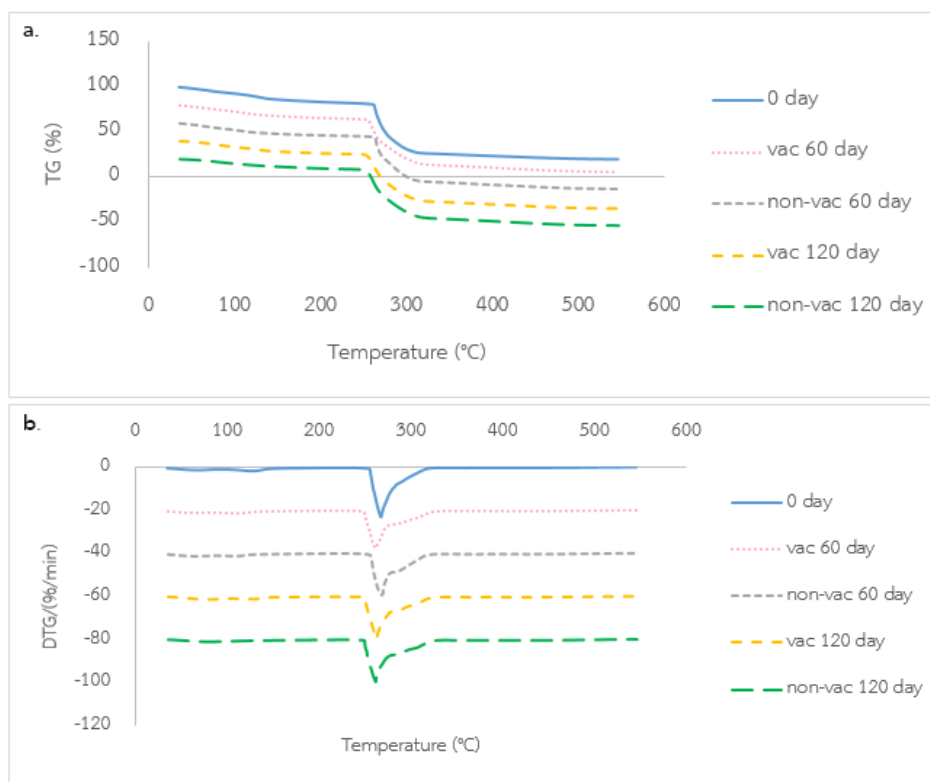


Figure 4.18 TGA (a) and DTG (b) thermograms of CO film after 0 day, 60 days in vacuum, 60 days in non-vacuum, 120 days in vacuum and 120 days in non-vacuum conditions

4.6.5 Fourier-transform infrared (FTIR) spectroscopy

The FTIR spectra of CO films at 0, 60 and 120 days in vacuum and non-vacuum condition shown in Fig. 4.19. All spectra showed the same pattern and confirmed the existence of CO in film. The intensity C=C peak of eugenol at 1514 cm^{-1} slightly declined over times related to the LC percentage result.

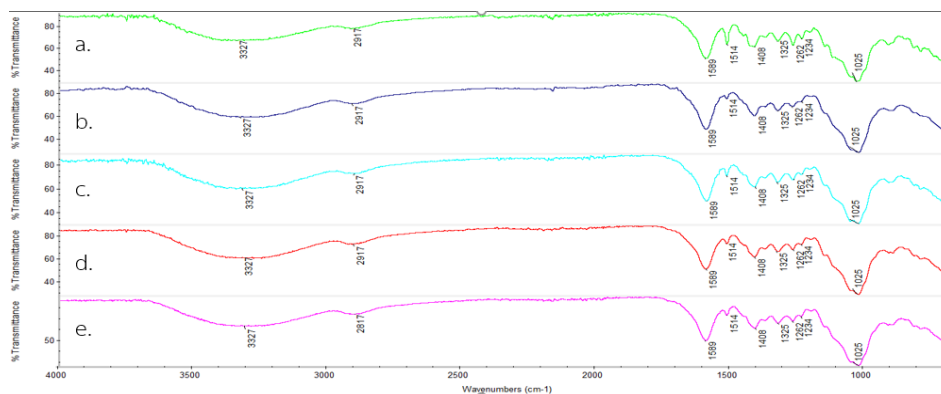


Figure 4.19 FTIR spectra of CO film at a) 0 day, b) 60 day in vacuum, c) 60 day in non-vacuum, d) 120 day in vacuum and e. 120 day in non-vacuum conditions


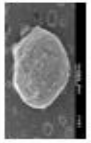


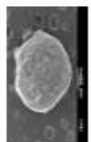
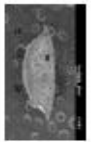






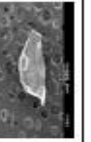

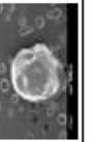
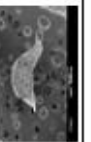



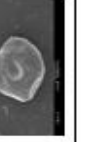




4.7 Stability of CO beads

4.7.1 Appearance and size

CO beads was gradually yellowed when were stored for 120 days in vacuum and non-vacuum condition (Table 4.4) due to the color change of clove oil. The size of bead was not significant difference ($p < 0.05$) after 120 days in both conditions.



Table 4.4 Appearance, size and SEM micrographs of CO film in vacuum and non-vacuum conditions.

Day	Vacuum				Non-vacuum			
	Appearance	Size (mm)	SEM Surfaces	SEM Cross-sections	Appearance	Size (mm)	SEM Surfaces	SEM Cross-sections
0		1.56 ± 0.03				1.56 ± 0.03		
15		1.50 ± 0.05	-	-		1.56 ± 0.03	-	-
30		1.49 ± 0.06	-	-		1.55 ± 0.03	-	-
60		1.51 ± 0.03				1.56 ± 0.02		
90		1.54 ± 0.04	-	-		1.56 ± 0.02	-	-
120		1.53 ± 0.11				1.50 ± 0.04		

4.7.2 Loading capacity percentage, SEM analysis and moisture content

The LC percentage of CO beads showed in Fig.4.20. The LC percentage of CO beads was not significant difference ($p < 0.05$) over time 120 days in both condition. From the graph, notice that the encapsulation of CO in each beads were inequitable. The vacuum storage was better than the non-vacuum storage wherewith the amount of clove oil in beads were greater. The cross-section image of CO beads was obtained dispersion of CO when stored for 120 days which observed from porous in CO beads (Table 4.4). The moisture of CO beads (Fig. 4.21) after 120 days was not significant difference ($p < 0.05$).

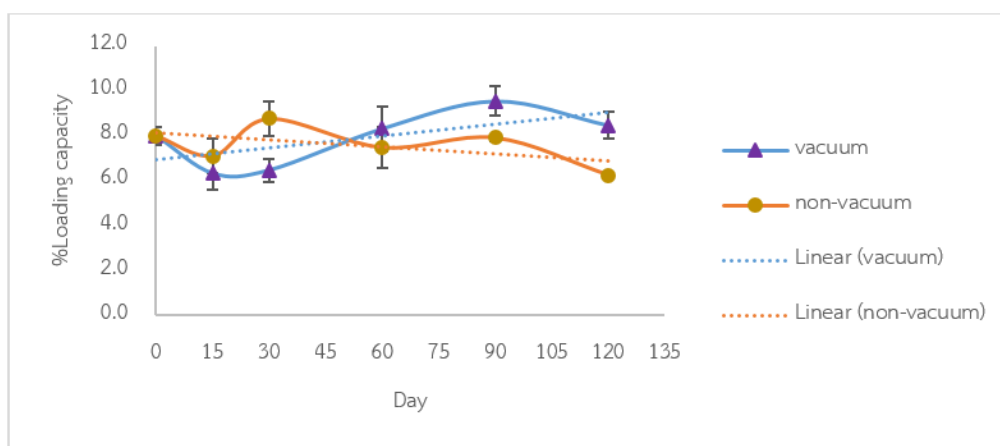


Figure 4.20 The %loading capacity of CO beads in vacuum and non-vacuum conditions

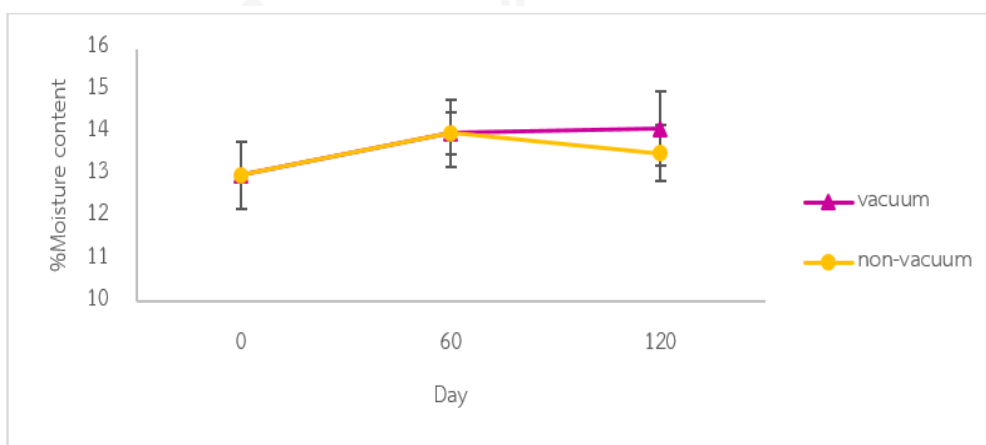


Figure 4.21 The moisture content of CO beads in vacuum and non-vacuum conditions

4.7.3 Fourier-transform infrared (FTIR) spectroscopy

The FTIR spectra of CO beads at 0, 60 and 120 days in vacuum and non-vacuum condition shown in Fig. 4.22. All spectra showed the same pattern and confirmed the existence of CO in film. The intensity C=C peak of eugenol at 1511 cm^{-1} .

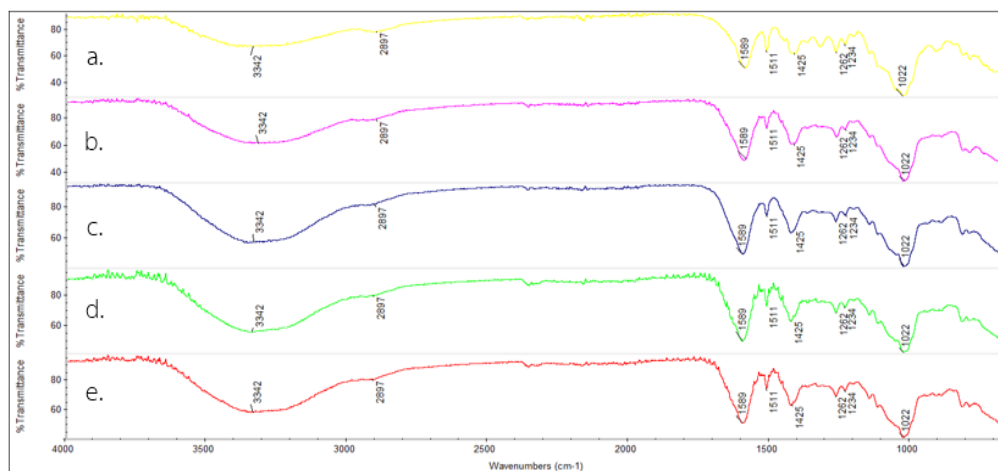


Figure 4.22 FTIR spectra of CO beads at a) 0 day, b) 60 day in vacuum, c) 60 day in non-vacuum, d) 120 day in vacuum and e. 120 day in non-vacuum conditions

CHAPTER V

CONCLUSION

This study reported the preparation of CO film and CO bead and expected to use as fish anesthetic. The CO film was fabricated by incorporating CO (2%) in the matrix of CMC (2%) and XG (0.8%). The components of the CO bead were 1% (w/v) of alginate, 0.5 % (w/v) of CMC and 0.5 % (w/v) of XG and 2% (w/v) of CO. The CO film and bead were consequently characterized the physical and chemical properties. The LC percentages of CO film and bead were 32.7 and 8.0, respectively. The SEM cross-section micrographs of both forms presented oil droplets dispersed in the polymer matrix. The FTIR and TGA analysis confirmed incorporation of CO in polymer matrix of both film and bead. The moisture content was 10% of CO film and 13% of CO bead. The CO films dissolved in the water faster than in the seawater because the ionic strength of medium inhibited the dissolution of polymer matrix. When CO film dissolved, the CO droplets in the matrix of polymers can disperse well in the medium. The CO beads swelled faster in the seawater but released faster in the water. The alginate swelled by ionic exchange between Ca^{2+} ion of bead and Na^+ ion of seawater. However, the ionic strength of the swelling medium decreased the water solubility of the hydrophobic CO. The CO in beads released up to 82% in water and 67% in seawater within 180 minutes and there was no separation between CO and the medium.

The shelf-life stability of CO film and bead was evaluated for as long as 120 days of the storage. The samples were kept in 2 conditions which were vacuum and non-vacuum sealed foil bags. The result showed that color of CO film and bead were gradually yellowed when stored for 120 days due to the color change of clove oil. The LC percentage of CO film gradually decreased within 60 days and after that the CO amount remained unchange and no difference between vacuum and non-vacuum conditions. The LC percentage of CO bead did not significant change after 120 days of

storage and storage in vacuum condition gave the higher LC percentage than that in non-vacuum condition.

In conclusion, the CO film can be used to prepare CO aqueous solution easier and faster than the CO bead. The CO film is the candidate prototype for further testing as fish anesthesia. However, the CO beads might be suitable for long-lasting fish anesthesia by control the release rate of CO.



REFERENCES

- [1] Charles, D.J. Antioxidant Properties of Spices, Herbs and Other Sources. 1 ed.: Springer-Verlag New York, 2012.
- [2] Uju, D.E. and Obioma, N.P. Anticariogenic potentials of clove, tobacco and bitter kola. Asian Pacific Journal of Tropical Medicine 4(10) (2011): 814-818.
- [3] Khunkitti, W., Veerapan, P., and Hahnvajjanawong, C. In vitro bioactivities of clove buds oil (*Eugenia caryophyllata*) and its effect on dermal fibroblast. International Journal of Pharmacy and Pharmaceutical Sciences 4(3) (2012): 556-560.
- [4] Shah, A., Jani, M., Shah, H., Chaudhary, N., and Shah, A. Antimicrobial Effect of Clove Oil (Laung) Extract on *Enterococcus faecalis*. Journal of Advanced Oral Research 5(6) (2014): 36-38.
- [5] Daniel, A.N., Sartoretto, S.M., Schmidt, G., Caparroz-Assef, S.M., Bersani-Amado, C.A., and Cuman, R.K.N. Anti-inflammatory and antinociceptive activities of eugenol essential oil in experimental animal models. Brazilian Journal of Pharmacognosy 19(1B) (2009): 212-217.
- [6] Manohar, V., et al. Antifungal activities of origanum oil against *Candida albicans*. Molecular and Cellular Biochemistry 228 (2001): 111-117.
- [7] El-Maati, M.F.A., Mahgoub, S.A., Labib, S.M., Al-Gaby, A.M.A., and Ramadan, M.F. Phenolic extracts of clove (*Syzygium aromaticum*) with novel antioxidant and antibacterial activities. European Journal of Integrative Medicine 8(4) (2016): 494-504.
- [8] Soto, C.G. and Burhanuddin. Clove oil as a fish anaesthetic for measuring length and weight of rabbitfish (*Siganus lineatus*). Aquaculture 136 (1995): 149-152.
- [9] Marking, L.L. and Meyer, F.P. Are better anesthetics needed in fisheries? . Fisheries 10(6) (1985): 2-5.
- [10] Schnick, R.A., Meyer, F.P., and Walsh, D.F. Status of fishery chemicals in 1985. The Progressive Fish-Culturist 48 (1986): 1-17.

- [11] Songkaew, A., Chokboonmongkol, C., Khattiya, R., Wongsathein, D., Mengumpun, K., and Pikulkaew, S. Induction time and behavior of anesthesia and recovery in Mekong Giant Catfish (*Pangasianodon gigas*) after anesthetized with clove oil and tricaine methanesulfonate (MS-222). Journal of the Thai Veterinary Medical Association under the Royal Patronage 58(2) (2007): 21.
- [12] Kildea, M.A., Allan, G.L., and Kearney, R.E. Accumulation and clearance of the anaesthetics clove oil and AQUI-S™ from the edible tissue of silver perch (*Bidyanus bidyanus*). Aquaculture 232 (2004): 265-277.
- [13] Administration, U.S.F.a.D. Select Committee on GRAS Substances (SCOGS) Opinion: Clove Bud Extract, Clove Bud Oil, Clove Bud Oleoresin, Clove Leaf Oil, Clove Stem Oil, Eugenol [Online]. 2015. Available from: <https://www.fda.gov/Food/IngredientsPackagingLabeling/GRAS/SCOGS/ucm261254.htm> [10]
- [14] Mylonas, C.C., Cardinaletti, G., Sigelaki, I., and Polzonetti-Magni, A. Comparative efficacy of clove oil and 2-phenoxyethanol as anesthetics in the aquaculture of European sea bass (*Dicentrarchus labrax*) and gilthead sea bream (*Sparus aurata*) at different temperatures. Aquaculture 246(1-4) (2005): 467-481.
- [15] Pirhonen, J. and Schreck, C.B. Effects of anaesthesia with MS-222, clove oil and CO₂ on feed intake and plasma cortisol in steelhead trout (*Oncorhynchus mykiss*). Aquaculture 220(1-4) (2003): 507-514.
- [16] Mitjana, O., et al. The efficacy and effect of repeated exposure to 2-phenoxyethanol, clove oil and tricaine methanesulphonate as anesthetic agents on juvenile Angelfish (*Pterophyllum scalare*). Aquaculture 433 (2014): 491-495.
- [17] Small, B.C. Anesthetic efficacy of metomidate and comparison of plasma cortisol responses to tricaine methanesulfonate, quinaldine and clove oil anesthetized channel catfish *Ictalurus punctatus*. Aquaculture 218(1-4) (2003): 177-185.
- [18] Mohammadi, M. and Khara, H. Effect of different anesthetic agents (clove oil, tricaine methanesulfonate, ketamine, tobacco) on hematological parameters

- and stress indicators of rainbow trout *Oncorhynchus mykiss*, Walbaum, 1792. Comparative Clinical Pathology 24(5) (2014): 1039-1044.
- [19] Hoseini, S.M. Efficacy of clove powder solution on stress mitigation in juvenile common carps, *Cyprinus carpio* (Linnaeus). Comparative Clinical Pathology 20(4) (2010): 359-362.
- [20] Iversen, M., Finstad, B., McKinley, R.S., and Eliassen, R.A. The efficacy of metomidate, clove oil, Aquí-S™ and Benzoak® as anaesthetics in Atlantic salmon (*Salmo salar* L.) smolts, and their potential stress-reducing capacity. Aquaculture 221(1-4) (2003): 549-566.
- [21] Javahery, S., Nekoubin, H., and Moradlu, A.H. Effect of anaesthesia with clove oil in fish (review). Fish Physiol Biochem 38(6) (2012): 1545-52.
- [22] Wongtavatchai, J., Rojsitthisak, P., Tipmongkolsilp, N., and Jongaroonngamsang, N. Formulation of clove oil solution as an anesthetic for aquatic animals. department of veterinary medicine Chulalongkorn University, 2006.
- [23] Cui, H., Zhao, C., and Lin, L. The specific antibacterial activity of liposome-encapsulated Clove oil and its application in tofu. Food Control 56 (2015): 128-134.
- [24] Mohammadi, M., Ramezani, M., Abnous, K., and Alibolandi, M. Biocompatible polymersomes-based cancer theranostics: Towards multifunctional nanomedicine. Int J Pharm 519(1-2) (2017): 287-303.
- [25] Shahavi, M.H., Hosseini, M., Jahanshahi, M., Meyer, R.L., and Darzi, G.N. Evaluation of critical parameters for preparation of stable clove oil nanoemulsion. Arabian Journal of Chemistry (2015).
- [26] Han, J.H. Innovations in Food Packaging 2ed. Edible films and coatings: a review, ed. Taylor, S.L.: University of Nebraska - Lincoln, USA, 2014.
- [27] Bourtoom, T. Edible films and coatings: characteristics and properties. International Food Research Journal 15(3) (2008): 237-248.
- [28] Schmidt, H. and Mennig, M. Wet coating technologies for glass [Online]. 2000. Available from: <http://www.solgel.com/articles/Nov00/mennig.htm>
- [29] Wong, M., et al. Large-scale self-assembled zirconium phosphate smectic layers via a simple spray-coating process. Nat Commun 5 (2014): 3589.

- [30] Sahu, N., Parija, B., and Panigrahi, S. Fundamental understanding and modeling of spin coating process : A review. Indian Journal of Physics 83(4) (2009): 493-502.
- [31] Katiyar, N. and Balasubramanian, K. Nano-heat-sink thin film composite of PC/three-dimensional networked nano-fumed silica with exquisite hydrophobicity. RSC Adv. 5(6) (2015): 4376-4384.
- [32] Saputra, A.H., Qadhayna, L., and Pitaloka, A.B. Synthesis and Characterization of Carboxymethyl Cellulose (CMC) from Water Hyacinth Using Ethanol-Isobutyl Alcohol Mixture as the Solvents. International Journal of Chemical Engineering and Applications 5(1) (2014): 36-40.
- [33] Dashipour, A., Khaksar, R., Hosseini, H., Shojaee-Aliabadi, S., and Ghanati, K. Physical, antioxidant and antimicrobial characteristics of carboxymethyl cellulose edible film cooperated with clove essential oil. Zahedan Journal of Research in Medical Sciences 16(8) (2014): 34-42.
- [34] Muppalla, S.R., Kanatt, S.R., Chawla, S.P., and Sharma, A. Carboxymethyl cellulose–polyvinyl alcohol films with clove oil for active packaging of ground chicken meat. Food Packaging and Shelf Life 2(2) (2014): 51-58.
- [35] Tesfay, S.Z. and Magwaza, L.S. Evaluating the efficacy of moringa leaf extract, chitosan and carboxymethyl cellulose as edible coatings for enhancing quality and extending postharvest life of avocado (*Persea americana* Mill.) fruit. Food Packaging and Shelf Life 11 (2017): 40-48.
- [36] Garc a-Ochoa, F., Santos, V.E., Casas, J.A., and Go mez, E. Xanthan gum: production, recovery, and properties. Biotechnology Advances 18 (2000): 549-579.
- [37] Nur Hazirah, M.A.S.P., Isa, M.I.N., and Sarbon, N.M. Effect of xanthan gum on the physical and mechanical properties of gelatin-carboxymethyl cellulose film blends. Food Packaging and Shelf Life 9 (2016): 55-63.
- [38] Guo, J., Ge, L., Li, X., Mu, C., and Li, D. Periodate oxidation of xanthan gum and its crosslinking effects on gelatin-based edible films. Food Hydrocolloids 39 (2014): 243-250.

- [39] Lee, K.Y. and Mooney, D.J. Alginate: Properties and biomedical applications. Progress in Polymer Science 37(1) (2012): 106-126.
- [40] Navarro, R., Arancibia, C., Herrera, M.L., and Matiacevich, S. Effect of type of encapsulating agent on physical properties of edible films based on alginate and thyme oil. Food and Bioproducts Processing 97 (2016): 63-75.
- [41] Harden, C.J., Craig Richardson, J., Dettmar, P.W., Corfe, B.M., and Paxman, J.R. An ionic-gelling alginate drink attenuates postprandial glycaemia in males. Journal of Functional Foods 4(1) (2012): 122-128.
- [42] Baghbani, F., Moztarzadeh, F., Mohandes, J.A., Yazdian, F., and Mokhtari-Dizaji, M. Novel alginate-stabilized doxorubicin-loaded nanodroplets for ultrasonic theranosis of breast cancer. Int J Biol Macromol 93(Pt A) (2016): 512-519.
- [43] Burckbuchler, V., et al. Rheological and structural characterization of the interactions between cyclodextrin compounds and hydrophobically modified alginate. Biomacromolecules 7 (2006): 1871-1878.
- [44] Mandal, S., Kumar, S.S., Krishnamoorthy, B., and Basu, S.K. Development and evaluation of calcium alginate beads prepared by sequential and simultaneous methods. Brazilian Journal of Pharmaceutical Sciences 46(4) (2010): 785-793.
- [45] Rehm, B.H.A. Alginates: Biology and Applications, ed. Steinbüchel, A. Vol. 13: Springer Dordrecht Heidelberg London New York, 2008.
- [46] Agarwal, T., Narayana, S.N., Pal, K., Pramanik, K., Giri, S., and Banerjee, I. Calcium alginate-carboxymethyl cellulose beads for colon-targeted drug delivery. Int J Biol Macromol 75 (2015): 409-17.
- [47] Soliman, E.A., El-Moghazy, A.Y., El-Din, M.S.M., and Massoud, M.A. Microencapsulation of Essential Oils within Alginate: Formulation and *in Vitro* Evaluation of Antifungal Activity. Journal of Encapsulation and Adsorption Sciences 03(01) (2013): 48-55.
- [48] Pasukamonset, P., Kwon, O., and Adisakwattana, S. Alginate-based encapsulation of polyphenols from *Clitoria ternatea* petal flower extract enhances stability and biological activity under simulated gastrointestinal conditions. Food Hydrocolloids 61 (2016): 772-779.

- [49] corporation, F. Alginate. in *FMC Biopolymer the science of formulation*. 2003: FMC Tower at Cira Centre South. 1-20.
- [50] Klangmuang, P. and Sothornvit, R. Barrier properties, mechanical properties and antimicrobial activity of hydroxypropyl methylcellulose-based nanocomposite films incorporated with Thai essential oils. Food Hydrocolloids 61 (2016): 609-616.
- [51] Ma, Q., Zhang, Y., Critzer, F., Davidson, P.M., Zivanovic, S., and Zhong, Q. Physical, mechanical, and antimicrobial properties of chitosan films with microemulsions of cinnamon bark oil and soybean oil. Food Hydrocolloids 52 (2016): 533-542.





APPENDIX

จุฬาลงกรณ์มหาวิทยาลัย
CHULALONGKORN UNIVERSITY

Appendix A

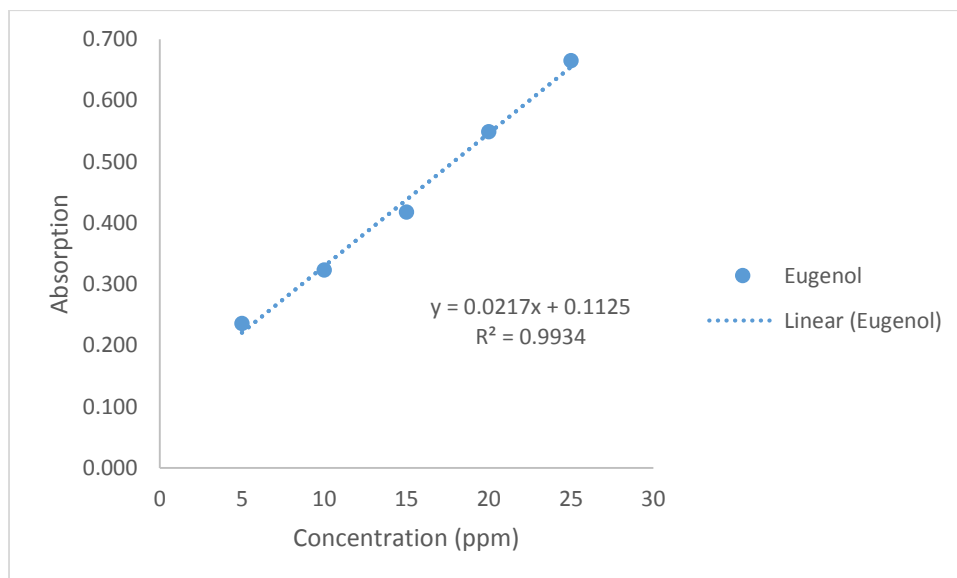


Figure A1 Calibration curve of CO by UV-visible spectrophotometer

Appendix B

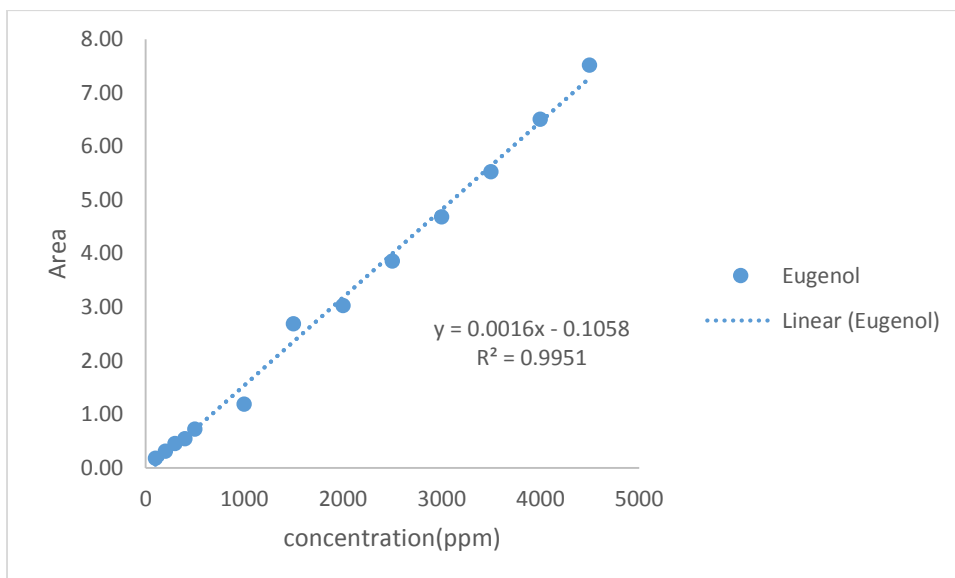


Figure B1 Calibration curve of CO by gas chromatography

Appendix C

Table C1 The color of CO film in vacuum and non-vacuum conditions within 120 days

Day	Vacuum				Non-vacuum			
	L*	a*	b*	ΔE	L*	a*	b*	ΔE
0	85.53±0.47	0.46±0.05	4.34±0.29	9.15±0.38	85.53±0.47	0.46±0.05	4.34±0.29	9.15±0.38
15	85.38±0.81	0.44±0.07	4.30±0.94	9.27±0.99	87.37±0.75	0.41±0.05	2.26±0.16	9.59±0.73
30	85.80±0.97	0.79±0.10	5.58±1.03	9.62±1.35	87.59±0.51	0.62±0.62	3.52±0.57	9.98±0.72
60	85.77±0.50	0.52±0.03	5.88±0.71	9.80±0.80	86.25±1.01	0.56±0.08	5.83±1.03	9.39±1.42
90	86.07±0.37	0.29±0.11	6.67±0.90	10.89±0.11	86.74±0.59	0.18±0.04	6.74±0.12	9.62±0.43
120	86.61±0.65	0.23±0.04	9.17±0.27	9.67±1.00	85.17±0.45	0.42±0.13	10.51±1.20	11.50±1.17

VITA

Name: Peewara Tungittibath

Date of birth: September 20, 1992

Nationality: Thai

Address: 3, Soi. Chonburibanbung 1, Chonburibanbung Road, Banbung, Bangbung, Chonburi, 20170

University Education: Bachelor's Degree from Department of Chemistry, Faculty of Science, Burapha University, 2010-2014. Master's Degree from Program in Chemistry, Faculty of Science, Chulalongkorn University.

Conference attendance: Poster presentation "Solubility enhancement of clove oil using polymeric blends" at The 40th National Graduate Research Conference. Higher Education Harmonization in Venue, PSU International Convention Center, Prince of Songkla University, Thailand, 20-21 October 2016.